UNIVERSITY OF HELSINKI

https://helda.helsinki.fi

Using the Taguchi experimental design for assessing within-field variability of surface run-off and soil erosion risk

Raza, Ahsan; Ahrends, Hella Ellen; Habib-ur-Rahman, Muhammed; Hueging, Hubert; Gaiser, Thomas

2022-07-01
Elsevier B.V.
http://hdl.handle.net/10138/573340
Raza, A, Ahrends, H E, Habib-ur-Rahman, M, Hueging, H & Gaiser, T 2022, 'Using the Taguchi experimental design for assessing within-field variability of surface run-off and soil erosion risk', Science of the Total Environment, vol. 828, 154567. https://doi.org/10.1016/j.scitotenv.2022.154567

Downloaded from Helda, University of Helsinki institutional repository. https://helda.helsinki.fi
This is an electronic reprint of the original article.
This reprint may differ from the original in pagination and typographic detail.
Please cite the original version.

Using the Taguchi experimental design for assessing within-field variability of surface run-off and soil erosion risk

Ahsan Raza[1,*], Hella Ahrends[2], Muhammad Habib-ur-Rahman[1], Hubert Hüging[1] and Thomas Gaiser[1]

[1]University of Bonn, Institute of Crop Science and Resource Conservation (INRES), Crop Science Group, Katzenburgweg 5, 53115, Bonn, Germany

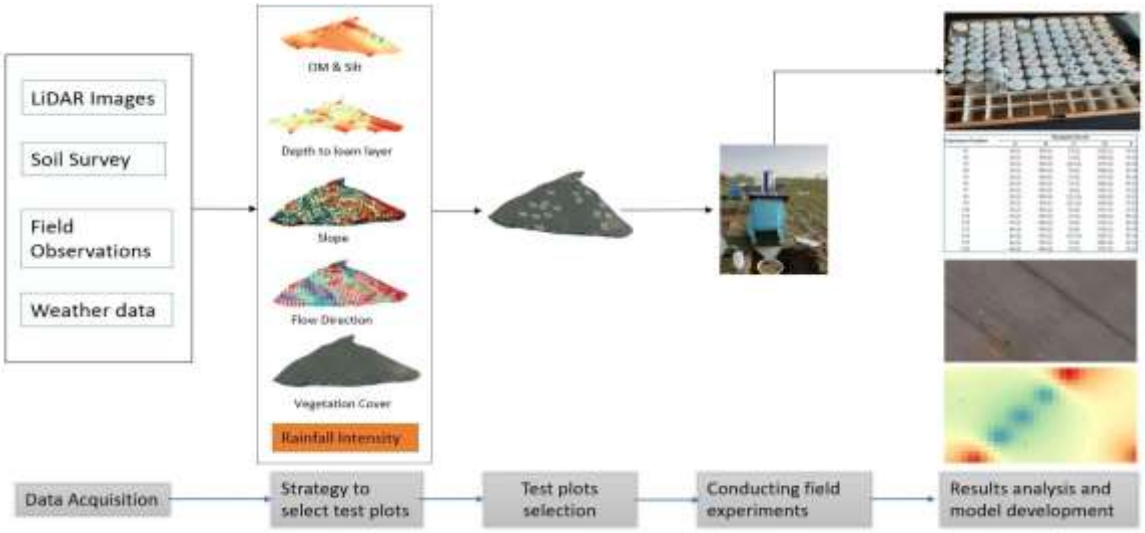
[2]University of Helsinki, Department of Agricultural Sciences, 00014 Helsinki, Finland;

***Correspondence: araza@uni-bonn.de; Tel.: +49(0)228 73-7200**

Highlights

- Taguchi's Fractional factorial experiment design approach was used to rank the factors affecting within-field soil erosion
- Signal-to-noise ratio analysis was used to identify optimum conditions for maximum sediment yield, runoff, and carbon and nitrogen content of sediments.
- Rainfall intensity contributed most strongly to erosion processes with 40.6 % followed by the slope (23.8 %).
- Applied workflow allowed for efficiently predicting soil erosion and identifying areas susceptible to soil loss at a high spatial resolution

Graphical abstract



Keywords: Design of experiment, heterogeneous field conditions, rainfall simulator, erosion-prone areas

Abstract

Water erosion is one of the soil degradation processes driven by environmental and field factors such as rainfall intensity, slope gradient, dynamics of vegetation cover, soil characteristics, and management practices. Most of the studies assess the separate contribution of these factors under controlled conditions. However, there is a lack of adequate knowledge regarding the complex interactions between prevailing factors and soil erosion processes under heterogeneous field conditions. This study investigated 16 combinations of 5 factors at 4 levels of each factor on the soil erosion process using Taguchi's fractional factorial experiment design, identifying the factor combinations resulting in maximum sediment yield, runoff, organic carbon, and nitrogen losses. We considered the factors: Soil organic matter and silt content (SiltOM), vegetation cover (VC), slope steepness (SS), rainfall intensity (RI), and depth to a loamy layer (DLL). The interactive effects of these factors and their combinations were visualized from the analysis of signal-to-noise (S/N) responses. Results indicated that interactions between the selected factors and soil erosion processes exist and multiple linear regression models were developed to predict sediment yields, runoff, carbon, and nitrogen losses at the sub-field scale. Results revealed that 1) RI with 40.6 % showed the highest contribution to sediment yield followed by SS (23.8 %), VC (17.74 %), SiltOM (14.77 %), and DLL (3.17 %), indicating a strong rainfall-erosion relationship; 2) the combination of levels of factors generating highest sediment yield was determined; 3) A simple multiple linear regression model developed for predicting local sediment yield showed the highest agreement with field observations (R^2=82.5 %). The findings suggest that Taguchi design could be used reliably for modeling soil erosion at field and sub-field scales. Using local calibration data such models have great potential for soil erosion risk assessments at the field scale, especially in areas where contributing factors and factor levels change at small spatial scales.

1. Introduction

Soil erosion by water has become a great concern all over the world (Keating et al., 2003; Krysanova et al., 2007). Soil erosion has significant impacts on environmental sustainability by adversely influencing agricultural production, water quality, and natural resources conservation (Issaka and Ashraf, 2017). It reduces the fertile soil depth and crop available soil moisture by the removal of essential nutrients and soil organic matter (SOM) and hence reducing the productivity of the soil (Jahun et al., 2015). Soil erosion by water is a form of land degradation resulting from multiple factors with complex interactions. Among others, these factors are rainfall intensity, runoff, small-scale soil heterogeneity in the vertical and horizontal direction, topography, and temporal variability of crop conditions (Václavík et al., 2013). Affected by heterogeneous environmental and field conditions, soil erosion involves complex processes that can strongly vary within single fields, in particular in undulated areas. (Cerdan et al., 2010). Therefore, identifying and categorizing the main causes of soil erosion at the field scale based on observations with a high spatial resolution for quantitatively assessing the spatial and temporal variability of soil erosion patterns are of great importance. Such information can provide support for decision-making for improved sub-field management and for farmers to avoid the degradation of fertile soils and for maintaining or enhancing crop productivity.

Numerous experimental and modeling studies have been conducted using approaches ranging from analytical to empirical techniques to gain a better understanding of runoff and soil erosion processes (Raza et al., 2021) and their potential outcomes (organic carbon and nitrogen losses, soil depth reduction, etc.,) under heterogeneous field conditions (Aga et al., 2020; Eslamian, 2014; J. R. Williams et al., 1984; Knisel and Nicks, 1981; Syvitski and Kettner, 2008; Viney and Sivapalan, 1999). Individual hydro-geomorphological processes and vegetation dynamics affect the soil erosion process differently depending on the scale (Aga et al., 2020; Nearing et al., 1999; Panagos and Katsoyiannis, 2019). In particular, soil physical properties such as soil structure, texture, bulk density, compaction, and soil thickness influence the erosion pattern and thus rate and magnitude of erosion (Ouyang et al., 2018; Ramezanpour et al., 2010). Other driving factors are the topography (i.e., slope gradient, slope length) and ground cover, which modify the physical forces and greatly impact hydrological processes (Liu and Singh, 2004). The amount, intensity, and frequency of precipitation are critical meteorological factors for surface runoff generation and soil erosion.

A few authors investigated the interactive impact of environmental and soil conditions on soil erosion. (Guidry et al., 2006; Sepaskhah and Bazrafshan-Jahromi, 2006) investigated the runoff and soil erosion under rainfall, varying slope, and soil factors, and found that the potentialities of both surface runoff and sediment yield varied with the level of rainfall erosivity but the impact differed among soil textures and slopes, indicating diverse nonlinearities of rainfall-runoff-soil factors-erosion relationships and their complex interaction. (Zambon et al., 2021) studied the dependency of soil erosion on soil surface conditions (seal formation) and soil types under controlled rainfall intensities. Under the same initial surface conditions, the erosion development for increasing rainfall intensity was almost consistent. (Warrington et al., 1989) noticed that increasing slope inclination tends to increase erosion, whereas removing surface crusts and increasing permeability rate led to decreasing surface runoff. (Gross et al., 1991) concluded that even low density vegetation coverage noticeably decreases the sediment yield with increasing rainfall intensities. However, different studies yield a different representation of erosion processes Differences in the results of the studies are mainly caused by the particular experimental conditions (selection of factors) and set-ups which affected the output. To date, there are a few attempts made to study the impact of multiple environmental and in-field factors to predict sediment yield and runoff, including, in some cases, carbon, and nitrogen losses under natural conditions (Anh et al., 2014; Li et al., 2017; J. H. Zhang et al., 2015). Most of these studies consider only one (Cerdà et al., 2021; Dunjó et al., 2004) or two (Ouyang et al., 2018; Ramos et al., 2019) factors to explain the erosion process and ignore the complex interaction of potential factors and specifically their in-field variability that may strongly affect the sediment yield and surface runoff. Most of these studies used defined rainfall intensities at plot scales to investigate soil erosion using a rainfall simulator.

Rainfall simulators and soil erosion plots are two widely used research facilities to assess and quantify the processes of soil erosion and sediment transport in overland flow (Sharpley and Kleinman, 2003). Different types of rainfall simulators with their specifications and sizes being optimized for specific pedo-climatic zones, topographies and land uses have been successfully applied in several field experiments (Barthès and Roose, 2002; Duiker et al., 2001; Fernández-Gálvez et al., 2008; Guidry et al., 2006; Lasanta et al., 2000; M. Sheklabadi et al., 2012; Sepaskhah and Bazrafshan-Jahromi, 2006; Srinivasan et al., 2007). However, many of these studies used standard plot sizes under controlled conditions (Albaladejo Montoro and Stocking, 1989; Raza et al., 2021; Renard et al., 1991) and with rainfall intensities far higher than the threshold for soil

detachment thus neglecting the interactions of modulated intensities and soil characteristics that can drive fine-scale spatial soil erosion processes (Kusumandari et al., 2021; Poulenard et al., 2001). In summary, there is still a lack of knowledge on the interactive effects of multiple factors and their potential levels on soil erosion processes under natural conditions that explicitly consider sub-field scale spatio-temporal dynamics**.** The quantitative knowledge is however of great importance for agricultural fields where management activities can lead to changes in the vulnerability of soils to erosion. Spatially explicit knowledge will help to understand within-field dynamics of erosion and sedimentation and greatly support precision agriculture by developing physical-based on empirical-based models. . Further, it provides quantitative validation data for high-resolution remote sensing data (such as unmanned aerial vehicle (UAV)-based Lidar measurements).

Most of the previous studies were conducted under controlled conditions with a limited number of factors, factor levels, and their interactions (Liu et al., 2019; Rieke-Zapp and Nearing, 2005; Sadeghi et al., 2017; Yusuf et al., 2016). Observing multiple factors and their complex interactions requires establishing several field experiments to disentangle their effects on spatial variation in soil erosion. Therefore, these studies used full factorial experimental designs to investigate the magnitude of the effects of factors on soil erosion that require a large sample size because it increases exponentially when all combinations of factors, factor levels, and interactions are considered (L. D. Meyer, 1981; Li et al., 2019; Meyer and Harmon, 1989). These designs are not applicable when the number of experimental runs is limited due to their cost- and labor intensity. To handle this challenge, the Taguchi method can be applied to any experimental study where the effect of up to ~30 factors on processes is studied while labor and cost intensity are minimized without lowering the quality of outputs (Taguchi, 1986). The Taguchi method is a type of general fractional factorial design, based on a selected number of factors and factor levels to identify the least number of experiments to be performed without compromising the overall output (Taguchi, 1987, 1986). So far, in an agricultural context, the Taguchi design mainly has been used for investigating the impact of fertilizer rates and plant density on cotton yields (Awty-Carroll et al., 2020; Chou et al., 2010; Ruchika Deo et al., 2007; Sivaiah & Chakradhar, 2019b). Further, it has been successfully applied to study soil erosion processes (Sadeghi et al. 2012, Mhaske et al. 2019) and results indicate similar performance compared with full factorial designs (Zhang et al. 2015, Zhang et al. 2021) and response surface methods (Moosavi & Sadeghi. 2021(F. Zhang et al.,

2015)). While providing evidence for the suitability of the design to study the effect of multiple factors on soil erosion, these studies only used a limited number of factors and their interactions. Further, runoff volume and resulting nutrient losses such as organic carbon and nitrogen from the field, which are critical variables for sustainable agriculture, were not investigated.

Encouraged by the successful application of this design in the studies mentioned above, we here use the Taguchi design to study fine-scale spatio-temporal dynamics of soil erosion processes (surface runoff, sediment yield, carbon and nitrogen losses) as affected by multiple factors at an agricultural field located in Western Europe under temperate climate conditions. More specifically, the objectives of this study are to

i. Investigate the within-field variability of the effects of the interaction between soil characteristics (soil organic matter (SOM), soil texture), topography (slope), rainfall intensity, and soil cover (field conditions) on soil erosion, surface runoff, carbon and nitrogen losses
ii. Quantify the percentage contribution of each of these five factors to soil erosion, surface runoff, carbon and nitrogen losses
iii. Develop empirical models to predict local runoff, sediment yield, carbon and nitrogen losses
iv. Identify erosion risk and sediment yield zones within the field

2. Methodology

2.1. Study area

The study was conducted on an agricultural field site located in the Löwenberger Land municipality, in the north of the federal state of Brandenburg, Germany (33U 374170E 5866893N) (Fig. 1). Brandenburg lies in the temperate, continental climate zone with mean annual temperatures between 7.8 °C and 9.5 °C and mean annual precipitation of ~ 600 mm (German Weather Service 2020, Ihinegbu & Ogunwumi, 2021). The research field comprises ~ 6.25 ha (Fig. 1). Terrain height averages around 51.5 to 57.5 m a.s.l. with north east facing gentle slope (Fig. 2). The soil was classified as Ferric Luvisol at up slopes (WRB, 2007) and in the marginal areas of the depression as Gley-Kolluvisol (Gleyic Anthrosol).

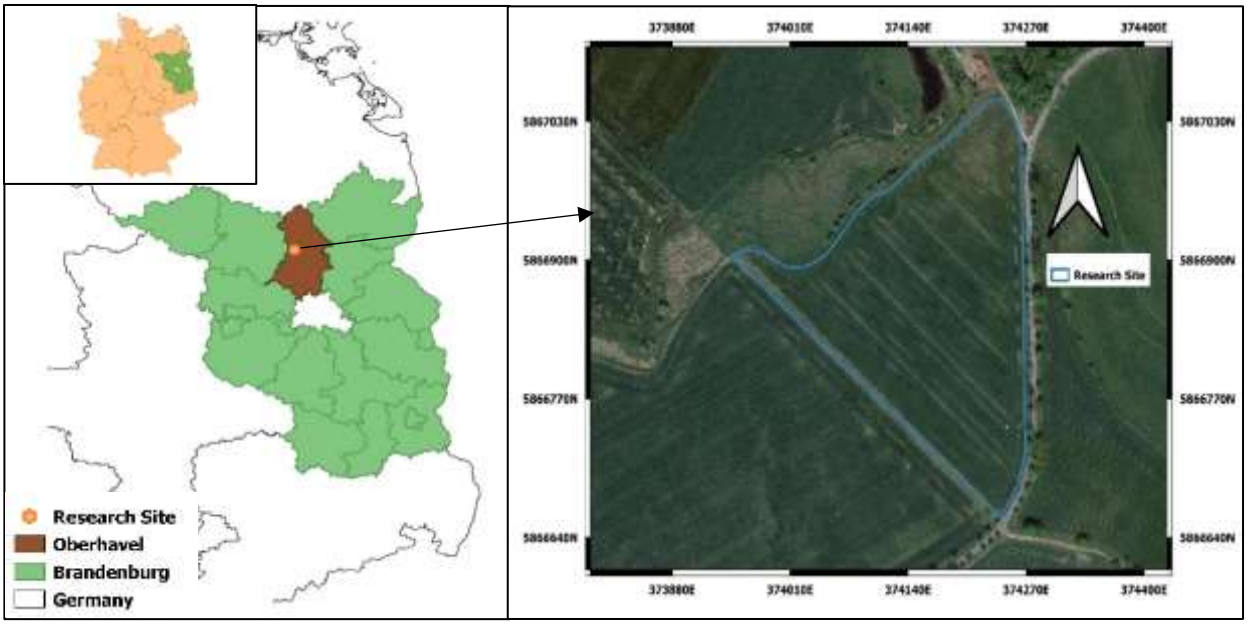


Fig. 1: Location of the study area (left) and an aerial image of the research field (May 8th, 2020, Google Earth)

2.2. Soil sampling

To characterize the spatial heterogeneity of soil characteristics soil augers (100 cm depth) were obtained from 87 different locations within the field (Fig. 2) in December 2019. At selected points, soil samples were analyzed for soil texture (proportion of silt, sand, and clay fractions) and SOM content, and the depth from the soil surface to a loamy layer. In soils derived from glacial deposits, the thickness of the sandy topsoil layers that are followed by a loamy layer, restricting vertical water movement compared to the sandy topsoil, is considered to increase the risk of water ponding at the soil surface and hence the risk of surface runoff and erosion. Samples were air-dried and sieved through a 2 mm mesh. Particle size distribution was determined with the Pipett method after SOM and carbonate destruction. Soil texture varied from silty loam to silt and medium sand according to the German soil taxonomy. According to Hofmann et al. (2016) and the soil taxation values in the German field cadastre of the state of Brandenburg (BB ATKIS), however, the topsoil is dominated by loamy sand.

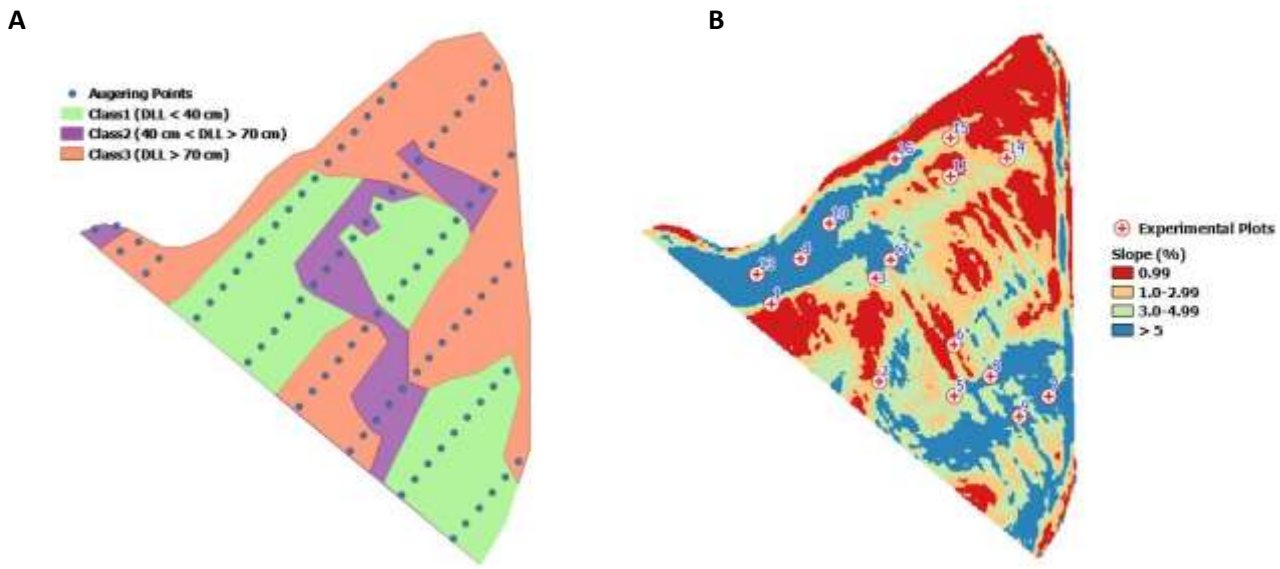


Fig. 2: Study site with soil augering points (A) and the locations of the rainfall simulation experimental plots (B, Numbers 1 to 16)

2.3. Experimental design

In contrast to classical statistical designs the "Taguchi design" is a type of general fractional factorial design, based on a selected number of factors and factor levels to identify the least number of experiments to be performed (Taguchi, 1987, 1986). The main factors and interactions that are most likely to be significant and the levels at which they are varied have to be defined in advance. Based on this knowledge Taguchi orthogonal arrays are selected with the choice depending on the tradeoff between time, resources, and quality of outputs (Medan et al., 2017; Rafidah et al., 2014; Woll & Burkhard, 2005). Subsequently to the experimental runs, the effect of each variable can be studied based on the signal-to-noise ratio (SN) (i.e., maximizing or minimizing SN ratios).

The Taguchi method systematically yields the best possible combination of factors and their levels to produce quality output at lower experimental cost and time. Based on the literature review (Chmelová and Šarapatka, 2002; P.U. et al., 2017; Pandey et al., 2007; Raza et al., 2021), For this study, five factors were selected: Sum of the percentage of silt and soil organic matter (SiltOM), vegetation cover (VC), slope steepness (SS), rainfall intensity (RI), and depth to loamy layer (DLL). For each factor, four levels are considered (Table 1). The ranges of these levels are based on soil surveys, site-specific scheduling of crop residue management (affecting vegetation cover), and the field topography derived from 2008 Lidar data with 1m spatial resolution

(https://geobroker.geobasis-bb.de). The selection of rainfall intensity levels is based on an analysis of 10-minute precipitation data provided by the German Weather Service for a nearby meteorological station (Brandenburg weather station (ID # 3552)) and adjusted to the capability and sensitivity of the mobile rainfall simulator (described below).

Table. 1: Experimental factors and their levels

Factor	Description	Unit	Level 1	Level 2	Level 3	Level 4
1	(SiltOM)*	%	> 20	18 - 20	16 - 18	< 16
2	vegetation cover	%	1 - 5 (C)	0 (B)	10 - 15 (E)	> 15 (L)
3	Slope steepness	%	< 1	1-3	3-5	> 5
4	Rainfall intensity	mm min^{-1}	< 2.5	2.7 - 3.3	3.4 - 4	> 4
5	Depth to loamy layer	cm	< 40	40 - 55	55 - 70	> 70

*the % of SiltOM decreases from level 1 to level 4, decided based on laboratory soil texture analysis. C, B, E, and L represent field conditions as cultivation, seedbed preparation, plant emergence, and Leaf development stage (3 Leaves unfold) respectively.

Due to the number of factors (5) and levels (4) as defined in Table 1, the orthogonal array L_{16} (4^5) for the Taguchi DOE was selected consisting of 16 experiments (factor combinations) (Table 2).

Table 2: Taguchi fractional factorial design L16 (4^5) used in this study

Factors \ Plot ID	Combination of levels					SiltOM (%)	Vegetation cover (%)	Slope steepness (%)	Rainfall intensity (mm min^{-1})	Depth to loamy layer (cm)
	1	**2**	**3**	**4**	**5**					
1	1	1	1	1	1	>20	1-5	<1	<2.5	<40
2	1	2	2	2	2	>20	0	1-3	2.7-3.3	40-55
3	1	3	3	3	3	>20	10-15	3-5	3.4-4	55-70
4	1	4	4	4	4	>20	>15	>5	>4	>70
5	2	1	2	3	4	18-20	1-5	1-3	3.4-4	>70
6	2	2	1	4	3	18-20	0	<1	>4	55-70
7	2	3	4	1	2	18-20	10-15	>5	<2.5	40-55
8	2	4	3	2	1	18-20	>15	3-5	2.7-3.3	<40
9	3	1	3	4	2	16-18	1-5	3-5	>4	40-55
10	3	2	4	3	1	16-18	0	>5	3.4-4	<40
11	3	3	1	2	4	16-18	10-15	<1	2.7-3.3	>70
12	3	4	2	1	3	16-18	>15	1-3	<2.5	55-70
13	4	1	4	2	3	<16	1-5	>5	2.7-3.3	55-70
14	4	2	3	1	4	<16	0	3-5	<2.5	>70
15	4	3	2	4	1	<16	10-15	1-3	>4	<40
16	4	4	1	3	2	<16	>15	<1	3.4-4	40-55

2.4. Plot selection

To select plot locations for experimental runs covering each of the 16 factorial combinations (Table 2), field maps on the depth to a loamy layer, slope inclination, and the sum of silt and OM were prepared, using SAGA within QGIS 3.16 (Fig. 3). Data on the depth to a loamy layer was derived from field surveys. Point data were spatially interpolated using ordinary kriging in SAGA. The topography was derived from 2008 LiDAR imagery (https://geobroker.geobasis-bb.de). Subsequently, map overlays were used to identify 16 plot locations. The 16 locations were considered to be well distributed in the research site (Fig. 2). At each location, rainfall simulator experiments were carried out at the respective intensity levels with 4 repetitions. To integrate the factors “vegetation cover”, simulations were performed on multiple dates with vegetation cover ranging from 0% (seedbed preparation), over 5% (cultivation) and 10% (crop emergence, DAS: 20) to >15% (leaf development stage 3, DAS: 204) (Table 3).

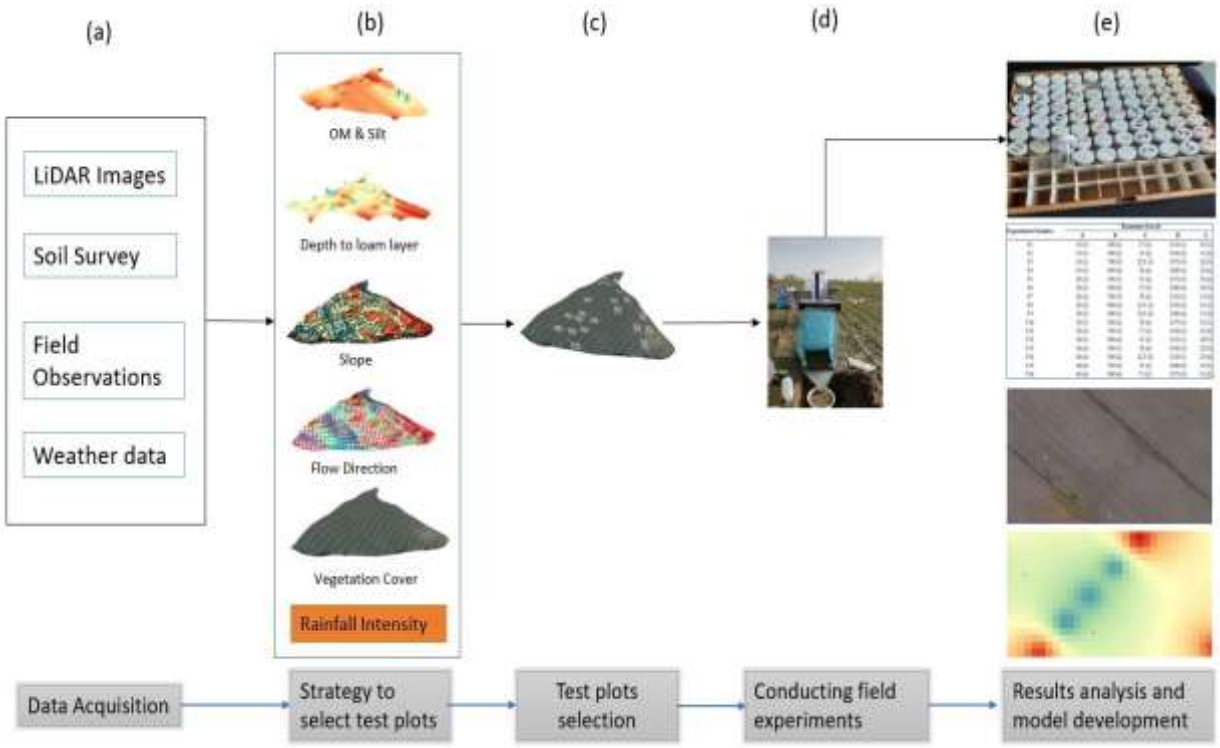


Fig. 3. Schematic diagram of the workflow for the rainfall simulation experiment: (a) Preprocessing of soil samples and remote sensing data (b) Preparing within-field factor levels for the Taguchi design (c) Selecting the locations of experimental plots (d) collecting sediments and runoff (e) Filtering and weighing sediment samples, runoff and CN concentration in sediments

2.5. Rainfall simulator

In this study, in order to generate targeted levels of rainfall intensity (Table 2), the portable non-pressurized rainfall simulator (Kamphorst, 1987) was used (Fig. 3d). The simulator was produced by Eijkelkamp (Eijkelkamp Agrisearch Equipment, Netherlands) and the design is owned by Wageningen University Research Centre. The ground coverage area is 0.0625 m^2 enclosed from three sides with stainless steel frame. The basic unit of the simulator consists of two Plexiglas containers connected with the frame. The upper container has a calibrated cylindrical reservoir having a capacity of 2300 ml. The lower container has 49 capillaries with a diameter of 0.6 mm. The basic unit is supported with four adjustable legs, 0.4 m average in height, on various slopes. Rainfall intensity is controlled by varying the atmospheric pressure inside the basic unit through an adjustable aeration pipe attached to the upper container. Fig. 3d illustrates the operation of the rainfall simulator in the field. Before the beginning of the experiments, the rainfall simulator was

calibrated in order to generate the four different rainfall intensities (Table 2) (Kamphorst, 1987; "Rainfall simulator - Field measurement equipment | Eijkelkamp," 2018). Each experiment was carried out for the duration of 8 minutes keeping in view the storage capacity of the reservoir and rainfall intensity levels. However, for the rainfall simulator, it is recommended to use it at the wettest season i.e., soil moisture content near to field capacity, when the soil surface is most vulnerable to erosion. For that purpose, a pre-wetting of the plot was carried out in the dry season. The water for pre-wetting is carefully applied through a plastic container with a perforated lid on it to avoid splash and runoff.

2.6. Sample preparation

The runoff from each plot and repetition and the corresponding sediment yields were collected in a 2L plastic bucket installed at the downslope end of the stainless steel frame of the simulator. The samples were thoroughly mixed by stirring before transferring them into plastic bottles. The volume of samples (runoff + sediment) was determined using glass flasks in the laboratory followed by wet sieving through a sieve with a mesh size of 2 mm. The samples were then placed in the oven at 60 ^{o}C for drying the dried samples and were later weighted to determine the sediment yield. There were no stones > 2 mm collected in any of the samples. A pycnometer with distilled water was used to determine the volume of sediments collected from each experimental plot (Benjeddou et al., 2017; Heiskanen, 2008). Surface runoff volume was calculated by subtracting the sediment volume from the total sample volume collected in the field. The sediment samples were then dried at 60 ^{o}C till samples were fully dried to prepare them for carbon and nitrogen (CN) analysis. The dried samples were transferred then into separate glass scintillation vials and analyzed for CN content by instantaneous oxidation of the sample via combustion with oxygen at an approximate temperature of 1020° C using an Elemental Analyzer Euro EA 3000 (EuroVector - RK Tech Ltd., Pavia)

2.7. Statistical analysis

In Minitab 17.0 software tool, signal-to-noise ratio analyses (SN) were used for the evaluation of experiment results (Chou et al., 2010; Sivaiah and Chakradhar, 2019). Three types of SN ratios are used (1) Nominal is better, (2) Higher is better, (3) Lower is better. Because the objective of this study is to identify the areas with the highest risk of erosion, "the higher the better (HB)" approach was used. The following equation was used to calculate the SN-ratio:

$$\frac{S}{N_s} = -10 * \log\left(\frac{1}{n}\sum\frac{1}{y^2}\right) \quad (1)$$

where, *n* represents the number of repetitions at each rainfall simulation plot, and *y* represents the studied variable. Here, *y* is sediment yield, runoff, nitrogen, or carbon content in the sediments from each experimental plot.

The statistical approach of analysis of mean (ANOM) was used to derive optimal conditions (Parr and Taguchi, 1989). ANOM is a graphical method for multiple group comparisons with an overall mean ("grand mean"). The mean $\frac{S}{Ns}$ ratio of each factor *I* at a specific level *i* (Eqn. 2) was determined using the following equation:

$$M_{Factor}^{Level} = \frac{1}{n_{Ii}}\sum_{j=1}^{n_{Ii}} \left[\left(\frac{S}{Ns}\right)_{Factor = I}^{level = i}\right]_j \quad (2)$$

In equation (2), n_{Ii} is the number of occurrences of factor *I* in level *i*. $\frac{S}{Ns}$ response figures and tables were obtained, and optimum conditions were established for each concerning output. J?

In addition, an analysis of variance (ANOVA) was used to investigate the influence of individual factors on sediment yield, runoff, and CN content (Cox et al., 2008). The percentage contribution of each experimental factor to the four output variables was estimated using the following equation:

$$\rho_F = \frac{SS_F - (DOF_F V_{ER})}{SS_T} \times 100 \quad (3)$$

Where V_{ER} is the variance of error, SSF is the factorial sum of squares, and DOF_F represents a degree of freedom obtained by subtracting one from the number of levels of each factor (*L*). The total sum of squares, SS_T, was calculated using the following equation:

$$SS_T = \sum_{j=1}^{m} \left(\sum_{i=1}^{L} Y_i^2\right)_j - mn\left(\overline{Y_t}\right)^2 \quad (4)$$

Y_t is obtained as:

$$\overline{Y_t} = \sum_{j=1}^{m} \left(\sum_{i=1}^{L} Y_i\right)_j / mn \quad (5)$$

Where, *m* represents the number of experimental plots covered in this study, and *n* represents the number of repetitions under the same experimental plot. The factorial sum of squares, SS_F, is given by:

$$SS_F = \frac{mn}{L}\sum_{k=1}^{L} \quad (\overline{Y}_K^F - \overline{Y_t}) \tag{6}$$

$\overline{Y}_K^F$ is the average value of the measurement results of a certain factor in the *kth* level. Furthermore, the variance of error, V_{ER} was given by:

$$V_{ER} = \frac{SS_T - (\sum_{F=A}^{D} SS_F)}{m(n-1)} \tag{7}$$

3. Results and discussion

3.1. Sediment yield

The variation of sediment yield depending on the five factors and their levels is shown in Fig 4A and 5A respectively. The average amount of sediment yield across replicates varies from 499.2 ± 20.6 to 60.5 ± 17.3 g m^{-2}. Plot-based rainfall simulation data show pronounced relative differences in sediment yield among different combinations of factors and their respective levels (Fig. 4A). Experimental plot B10 (0 % vegetation cover, a rainfall intensity of 3.4-4 mm min^{-1}, the slope of 4 %, SiltOM 16-18% of and DLL of < 40cm) shows the highest sediment mass with 499.2 g m^{-2}, indicating the highest erosion levels under these conditions. The lowest sediment mass (60.5 g m^{-2}) was obtained at plot L12 (vegetation cover was >15 %, rainfall intensity < 2.5 mm min^{-1}, and slope between 1 and 3 %). Fig 5 shows the means of sediment yield for each factor and each level and compares them to the overall factor mean (grand mean, dashed line) (ANOM). These graphs show that the amount of sediment increases with an increase in rainfall intensity (Fig. 5A). The minimum rainfall intensity needed to initiate soil erosion, in this study, was 2.5 mm min^{-1}. At lower rainfall intensities, the infiltration rate is higher in the beginning. The potential kinetic energy of raindrops is small and the splash effect is weak and so is the sediment yield. In addition, runoff volume is relatively small under lower rainfall intensities (Mohamadi and Kavian, 2015). The relationship between rainfall intensity and sediment yield varied across intensity levels in a systematic way (Fig. 5A). The sediment yield increased to 204.9 g m^{-2} when the RI increased to level 2, which was 73.5 g m^{-2} higher than at RI level 1. The increment was 253.3 g m^{-2} and 310.7 g m^{-2} with RI levels 3 and 4 respectively, where sediment yields were respectively 1.9 and 2.4 times higher than at RI level 1 (Fig. 5A). This result may indicate that at the plot scale, soil loss

would linearly increase up to a threshold of rainfall intensity, beyond which soil loss would increase non-linearly. Similarly, (Kandel et al., 2004) found a non-linear relationship between high-intensity rainfall and soil erosion processes. Therefore, it can be suggested that high rainfall intensities resulted in greater soil losses. This is also confirmed by other studies where high intensity rainfall events increased sediment yield (Jebari et al., 2008; Sukartaatmadja et al., 2003; Ziadat and Taimeh, 2013a) and sediment transport.

Soil detachment and runoff significantly increased with rainfall intensity for both uncultivated and cultivated lands (Ziadat and Taimeh, 2013b) but the level of vegetation cover has a significant effect on the soil detachment. As for plot B10, the same rainfall intensity of 3.4−4 mm min^{-1} was applied to plots E3, C5, and L16 producing 188.1 g m^{-2}, 207 g m^{-2}, and 199 g m^{-2} average sediment yield respectively (Fig. 4). However, in plot B10 the sediment yield was 499.2 g m^{-2}. Among the rates of sediment yield for four vegetation covers analyzed in this study, vegetation cover level 4 was found most beneficial for preventing soil losses. The eroded sediment yield was below 149 g m^{-2} when the vegetation cover was more than 15 % (level 4). The sediment yield generally tended to decrease with an increase in vegetation cover (Table 3). The highest mean sediment yield (averaged across all other factors) was observed after seedbed preparation (vegetation cover 0 %) with 292.16 g m^{-2} (Fig. 5A). In this study, increasing vegetation cover dramatically reduces sediment yield which is in accordance with the results of (Donjadee and Chinnarasri, 2012; Lin et al., 2018). (Zapata et al., 2021) mentioned that the vegetation cover interception reduces the diameter of the drops reaching the soil surface and hence reduces the kinetic energy of a raindrop. (Huang et al., 2012) also described that vegetation cover increases soil surface roughness that acts as a barrier to impede surface runoff and increases infiltration time. Thus, vegetation cover reduces the sediment yield by reducing the kinetic energy of raindrops, intercepting rainfall, increasing surface roughness, and enhancing infiltration times.

A positive relationship was further detected between slope and sediment yield. The sediment yield increased from 162.24 g m^{-2} at a slope of 1 % to 297.44 g m^{-2} at a slope of 5 % Fig. 5A. Previous studies also show that the sediment yield increases with increasing slopes. This indicates a strong positive relationship between slope and sediment yield (Grismer, 2012). Under extreme rainfall intensities, it has been observed that surface runoff velocity and sediment yield are primarily driven by slope inclination (Yan et al., 2018). These observations are likely related to higher overland flow velocities at higher slope gradients (Defersha and Melesse, 2012) resulting in higher sediment

yield. A gentle slope is less subject to activation and transportation of eroded sediments. Additionally, the splashing effect of raindrops generates surface sealing on gentle slopes producing more surface runoff carrying sediments. Soil particles are detached from the steep slopes where downward gravity is comparatively large. Therefore, there is a tradeoff between rainfall intensity and slope gradient. (Wu et al., 2018b) proved that rainfall intensity has more influence than slope gradient on sediment yield.

The surface soil texture also governs the sediment yield under varying rainfall intensity events. Water availability and water holding capacity are largely dependent on the texture of the soil profile, especially under rain-fed conditions (Libohova et al. 2018; Wang et al. 2020; Zhou et al. 2020). The decreasing concentration of SiltOM in the surface soil showed an increasing trend in sediment yield except for level 4 (2.5 %) which produced a mean sediment yield of 263.52 g m^{-2} which was slightly lower than at level 3 (275.84 g m^{-2}). The detachment of soil is mainly affected by the size and weight of soil particles, organic matter, and the kinetic energy of the raindrops (Sadeghi et al., 2017). The silt content varies from 10.2 to 19.5 % in the study area. The loose particles of silt showed a higher tendency to detachment and erosion process. Soil erodibility increases with increasing silt content (Baruah et al., 2019) but it reduces drastically once the crust is formed. However, SiltOM explicated the strong negative effects of mean weight diameter on splash erosion, and the indirect impact of high organic matter (> 2%) on splash erosion by improving the aggregate stability (Sun et al., 2021). Moreover, With high rainfall intensity and longer test duration, detaching capacity was achieved faster and a surface seal appeared on the soil surface (Michel et al., 2014).

3.2. Surface runoff

At different growth stages of the crop, the runoff process at different rainfall intensities, slope gradients, and soil textures are shown in Fig. 4B. The observed mean runoff volume varies between 23.5$\pm$1.07 and 6.54$\pm$0.62 mm among the plots. The plots where rainfall intensity level 4 was applied showed 42.5 % more surface runoff compared to those plots with rainfall intensity level 1. The increase of runoff in the low rainfall intensities was gentle and later it tend to be large. In general, for the highest rainfall intensity, the recorded runoff depth varied from 23 mm to 17.2 mm. On the other hand, for the events with the lowest rainfall intensity, the recorded runoff depth varied from 10. 4 to 6.8 mm. According to the comparison with local meteorological data from the closest

weather station, these two classified intensities can be termed as moderate rainfall intensity events and high-intensity storm events respectively. Both of which can produce surface runoff on local slopes in the study area. In our simulation experiments, the rainfall intensity shows a positive relationship with the depth of surface runoff under all vegetation covers. The high rainfall intensity occurring in short duration results in a higher runoff depth (Krisnayanti et al., 2021). The diameter and threshold raindrop velocity tends to increase with higher intensity rainfall. This event is particularly noticeable when the rainfall intensity is at level 4. Heavy raindrops provide more kinetic energy which changes the surface roughness producing pores blockage and soil crusts, which yield higher surface runoff (Lu et al., 2016).

The increasing surface runoff depth is positively related to rainfall intensity at the same slope inclination level and displayed order of 2.5 mm min^{-1} <2.7-3.3 mm min^{-1} < 3.4-4 mm min^{-1} <4 mm min^{-1} (Fig. 5B). However, the analyses of the relationship between slope gradient and runoff show increasing surface runoff were observed when the slope increased from 1−3 % (level 2) to >5% (level4) with runoff depth of 10.66 mm and 15.93 mm, respectively. However, it was decreased from 13.573 mm to 10.66 mm despite an increasing slope gradient from <1 % (level 1) to 3 % (level2) and also dropped to 15.08 mm when the slope was >5 % (level 4). The main reason is that observations at slope levels 1 and 2 are performed for soil class 1 and class 2, with high and moderate permeability, respectively (Fig. 2A). Previous studies also indicate that surface flow decreases with increasing slope gradient as the rain-bearing area becomes small as at smaller slope gradient the infiltration time is longer at the beginning with high permeable soil conditions (Deng et al., 2019; Wu et al., 2018a). Also, other studies show that surface runoff increases and tend to stabilize with the further increase of the slope gradient (Zhong and Zhang, 2011) but some studies also show that runoff increases first and then start decreasing with increasing slope gradient (Jourgholami et al., 2021; Li et al., 2020; Li and Yu, 2012). The present study shows similar results. Guo et al., (2018) showed that runoff depth is directly related to rainfall intensity and in a negative relationship with slope gradient. Infiltration rates decrease as slope increases from 6° to 35° and, thus, runoff depth increases to a certain extent until a critical slope gradient of 11° is reached at which infiltration rate trend starts changing (Liu et al., 2015). With further increments in slope, the runoff depth gradually decreases (Jourgholami et al., 2021; Nassif and Wilson, 1975). The rainfall intensity has more impact on runoff than slope gradient in this study which is in line with the work

by (Wu et al., 2018b). Since the slope gradients at our research site are well below 10 degrees the stronger impact of rainfall intensities agrees with other studies (Liu et al., 2015)

In this study, vegetation cover had a positive relationship with runoff depth. Fig. 5B shows that from level 1 (1-5 %) to level 2 (0 %) of vegetation cover there is an abrupt increase in surface runoff as on bare soil there are no interception losses. Then the runoff depth increases with increasing vegetation cover from level 3 (10-15 %) to level 4 (>15 %). The runoff depth was in the order of level 4 > level 2 > level 3 > level 1 of vegetation cover for both high and low rainfall intensity and all slope gradients. However, many studies show that runoff decreases with increasing vegetation cover due to higher canopy interception and rain redistribution reduces energy and runoff depth (He et al., 2020; Loch, 2000; Meng et al., 2007; Tong Li et al., 2020). The reason for high runoff depth at high vegetation cover can be hydrophobic repellency (De Jonge et al., 2007; Hermansen et al., 2019; Knadel et al., 2016) of the surface soil, as higher vegetation cover extracts more soil water. In fact, low soil moisture conditions under higher vegetation cover as noted during the field experiments. Many studies have reported that surface runoff depth increases under dry conditions such as drought periods (Burch et al., 1989; Buttle and Turcotte, 1999; Gomi et al., 2008; Sosa-Pérez and MacDonald, 2017). These studies suggested that the generation of hydrophobic soil surface conditions was one of the main reasons for this phenomenon under dry conditions. (Burch et al., 1989) for example, found that runoff depth increases from 5 % to 15 % due to the hydrophobic conditions after drought or dry summer. These previous studies suggest that because of drought development water repellent soil surface conditions produce more surface runoff regardless of high vegetation cover. The size of the plot can also have a significant impact on the runoff depth. Results obtained by Smets et al. (2008) indicate that there is significant variation in the effectiveness of vegetation cover on runoff if the plot is less than 11m long. Plot scale significantly affects the influence of surface roughness and vegetation cover on sediment yield and runoff depth (Jourgholami and Labelle, 2020).

The runoff depth changed with changing silt and organic material content among plots and results suggest that effects are significant ($p < 0.027$). The results agree with Vaezi et al. (2010), who also observed that runoff significantly correlated with silt ($p < 0.001$) and organic material ($p < 0.05$). Organic material positively affects the soil permeability, hence reducing the surface runoff depth (Sepaskhah and Bazrafshan-Jahromi, 2006). A similar pattern was observed for levels 1, 2, and 4 of this factor with the runoff averaging 14.05 mm, 13.82 mm, and 12.50 mm, respectively. Slightly

increasing runoff depth at level 3 was observed. Results agree with studies indicating that the primary factors affecting surface runoff during rainfall simulation experiments are current soil moisture levels, soil texture, slope, and rainfall intensity (Wang et al., 2016; Ziadat and Taimeh, 2013b). The highest runoff was recorded with 23 mm at plot B10 where SiltOM was at level 3 (Fig. 4) (Table. 4) and depth to loamy layer < 40 cm (Fig. 2). Later the runoff depth tends to decrease to 12.4 mm as SiltOM percentage increases in the field to level 4. A general trend in this study depicts that with increasing SiltOM content there is a decrease in surface runoff depth with a slight difference at level 3 The depth to a loamy layer (DLL) may act contrary to the effect of the silt content on runoff depth. A thicker sandy topsoil (i.e. deeper depth to loamy layer) may positively affect the soil permeability increasing the infiltration and consequently reducing the surface runoff depth. Thus, spatial variation in these soil properties in the study area noticeably influences the runoff generation in the test plots. This has been also proved in previous studies (Brakensiek and Rawls, 1994; Hrabovskỳ et al., 2020; Meena et al., 2020) mentioning that spatial variability of infiltration capacity is related to the spatial variability of topsoil characteristics that consequently affect the runoff generation.

3.3. Carbon and Nitrogen concentration in sediment yield

Soil carbon and nitrogen concentration redistribution is strongly governed by the amount of detached sediment within cultivated lands and it is generally accepted that C and N are preferentially transported during soil erosion (Holz and Augustin, 2021). The average values of carbon and nitrogen losses under each level of vegetation cover, slope, and rainfall intensities are presented in Fig. 4C & 4D respectively. Nitrogen and carbon contents of observed sediment yields are highly correlated and vary among experimental plots (Fig 4. C & D). Total C and N losses ranged between 12 ± 1.02 to 3.29 ± 0.496 g m^{-2} and 0.948 ± 0.073 to 0.106 ± 0.016 g m^{-2} respectively with moderate to high standard deviation, depending on RI, vegetation cover percentage, and SiltOM content (Fig. 4. C & D). As reported for the soil loss, C and N losses on the plots were positively related to the rainfall intensity ranging between 2.8 to 7.7 g m^{-2} and 0.2 to 0.4 g m^{-2} (Fig. 4).

In Figure 5C and 5D, it is obvious that the highest nutrient losses were found at vegetation cover more than 0 % despite other land covers percentages contributing less to the nutrient losses (Fig. 5. C & D). However, C and N losses were higher in at a vegetation cover of 15 % and in barren

509 land when the soil was subjected to rainfall intensity level 4 (4 mm min^{-1}) (Fig. 4. C & D). This
510 behavior is related to the absence of topsoil protective cover that reduces the impact of raindrops
511 and detachment of soil particles (Nunes et al., 2011). The highest C loss was found under RI of >
512 4 mm min^{-1} with values ranging between 12$\pm$1.02 g m^{-2} and 7.68 $\pm$1.12 g m^{-2} after 8 min rainfall,
513 respectively for vegetation cover levels 4 and 3 (Fig. 5C). Regarding N losses, the highest losses
514 were recorded in the plots with the highest C losses. The smallest C and N loss was observed as
515 2.8 and 0.2 g m^{-2} respectively at low rainfall intensities when detachment forces were small (Fig.
516 5. C & D). The experiments carried out in this study confirm the soil susceptibility to loose nutrients
517 under specific vegetation cover, even at a low rainfall intensity level (< 2.5 mm min^{-1}). All the
518 study plots have varying silt and organic matter contents, which made soils to lose nutrients
519 defining crusting indexes (Awadhwal and Thierstein, 1985). The different values of runoff induce
520 differences in sediment yield and transport of nutrients. Higher rainfall intensities produce higher
521 runoff depth. It could be confirmed that nutrient losses increase exponentially with higher rainfall
522 intensities. The analysis of slope gradient effect on nutrient loss, where higher soil losses occur,
523 shows that soil sealing can be the main factor that limits runoff as it does not increase significantly
524 with increasing slope (Fig. 5B) (Ramos et al., 2019). However, as sediment yields are increasing
525 with an increasing slope so do the C and N losses captured in the collected sediments except at
526 slope level 3 where C and N losses are reduced as slope increases from level 2 to level 3. The
527 reason is probably that the plots with slope level 3 lie in soil class 3 with throughout sandy texture
528 and lower C and N concentrations in the topsoil (Yost and Hartemink, 2019). The results suggest
529 that a permanent vegetation cover is essential to reduce C and N losses.

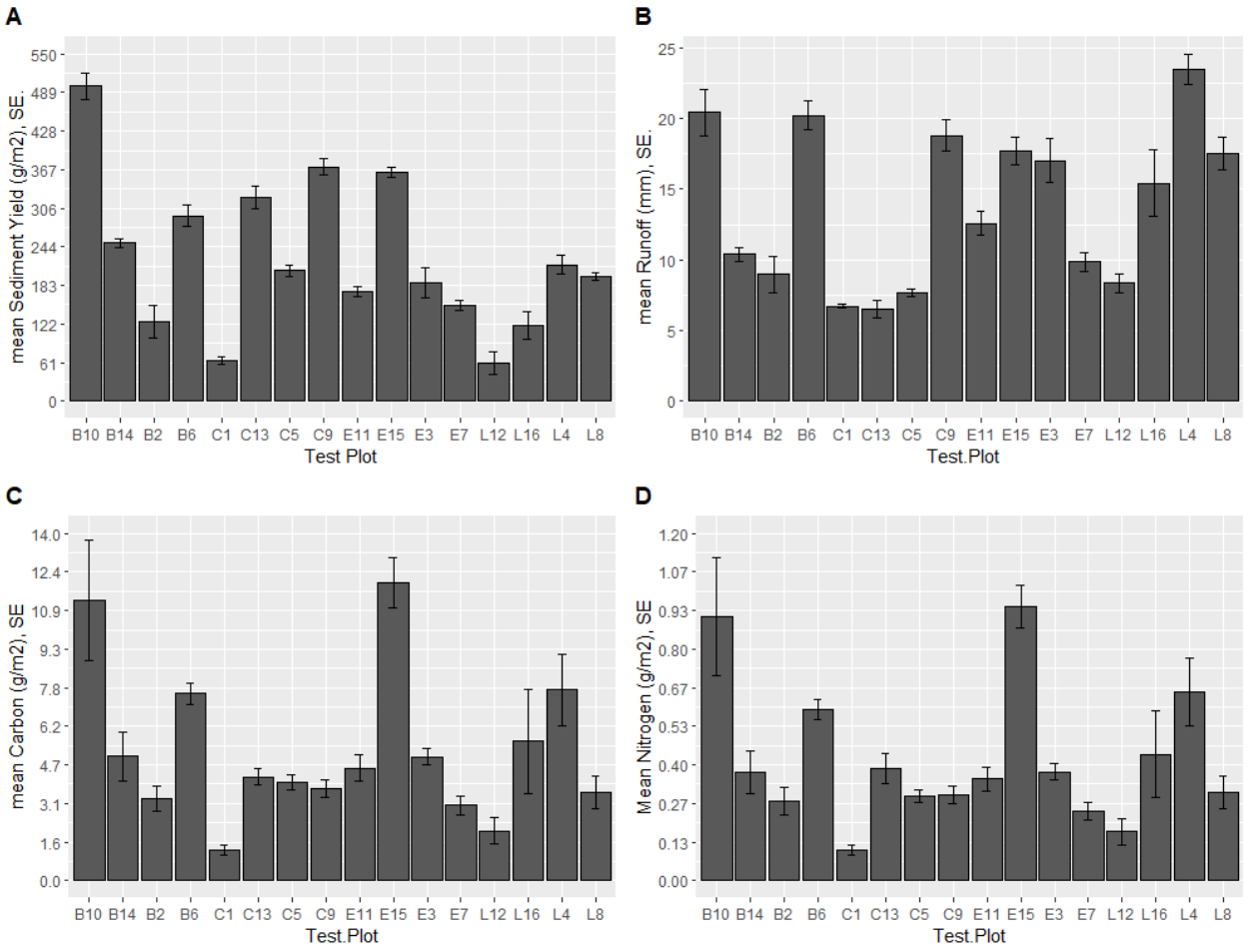


Fig. 4: Mean temporal variations and standard error (SE) in sediment yield, runoff, carbon, and nitrogen in relation to heterogeneous field conditions

Table 3: Mean sediment yield observed under changing soil surface conditions (vegetation cover factor levels)

Field condition	Vegetation cover	Mean sediment yield	Standard error
	%	g m^{-2}	g m^{-2}
Cultivation	5	241	31.1
Seedbed reparation	0	292	35.8
Emergence stage	10	219	22.5
Leaf development (3 Leaves unfold)	15	149	17.7

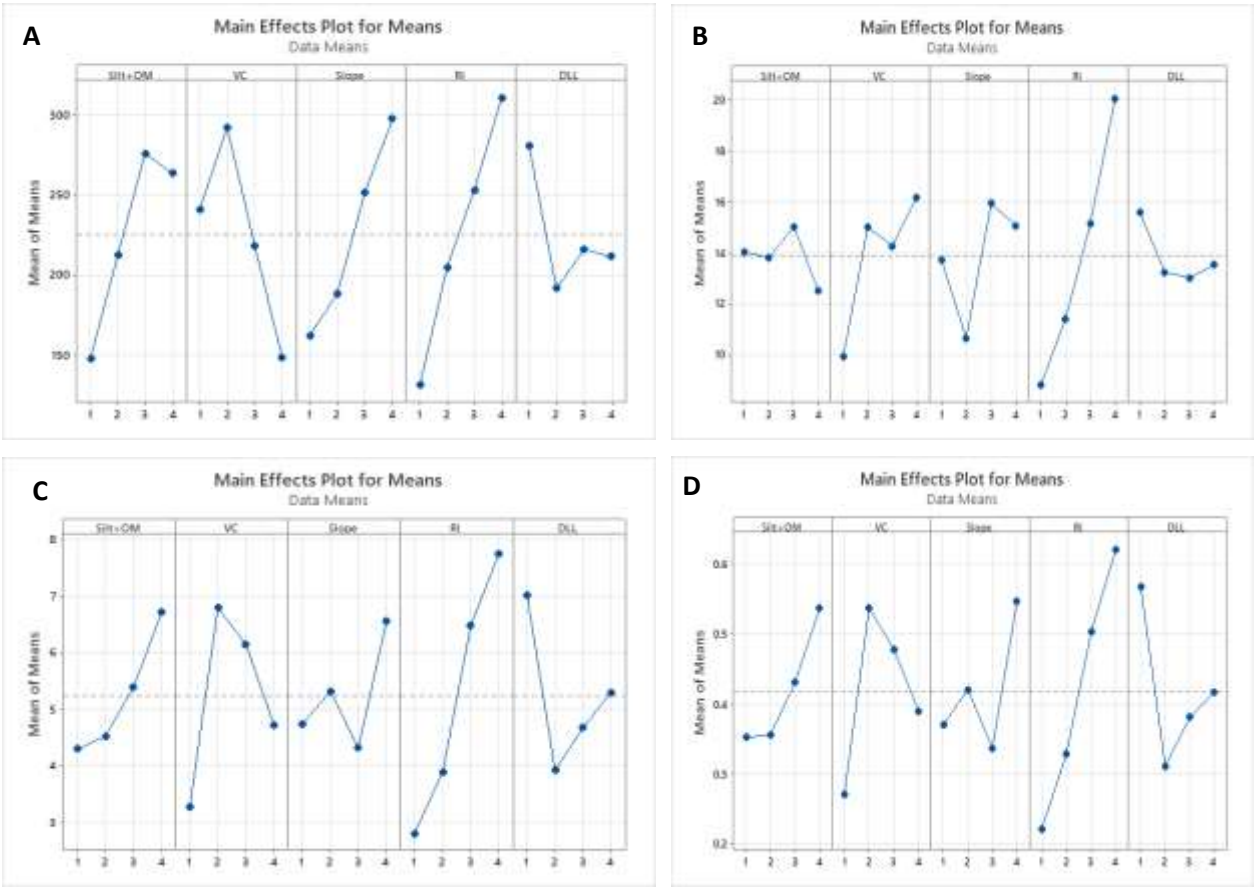


Fig. 5: Analysis of means (ANOM)) for A: Sediment yield (g m^{-2}), B: Runoff (mm), C: Carbon (g m^{-2}), D: Nitrogen content (g m^{-2}). Mean values for each level of each factor (blue dots) and the overall mean of each factor (dashed green line) are shown.

3.4. Optimal conditions for maximum sediment yield, surface runoff, Nitrogen, and Carbon content

The obtained S/N ratio responses for sediment yield, surface runoff, carbon, and nitrogen content are shown in Table 4 and Table 5. A Higher S/N ratio implies low variations between the desired output and the measured output. The maximum S/N ratio values among the 16 experiments, indicated in table 4 were 53.97 for sediment yield and 26.21 for runoff, 21.59 and -0.81 for C and N losses respectively in the test plot 10 with factor combination of $SiltOM_3$-VC_2-SS_4-RI_3-DLL_1 (Table 4). Inserting these values from table 4 into Eqn. 2 resulted in mean values of S/N ratios for each factor level. The maximum values of means of the S/N ratio were then identified. The bold values in Table 5 show the factor level with the highest S/N ratio for each factor and output variable (sediment yield, runoff, C and N losses). The highest mean S/N ratio for sediment yield was

obtained at factor level 4 for SiltOM, SS, and RI, at level 2 for VC, and level 1 for DLL (Table 5). Thus, we can predict that the highest sediment yield should be obtained with the factor level combination $SiltOM_4$-VC_2-SS_4-RI_4-DLL_1 (Table 5). On the other hand, the lowest sediment yield should be obtained with the factor combination $SiltOM_1$-VC_4-SS_1-RI_1-DLL_2. The estimated optimum factor level combination for obtaining the highest surface runoff was found to be $SiltOM_3$-VC_4-SS_3-RI_4-DLL_1 (Table 5). The highest rainfall intensity (>4 mm min^{-1}) led to the highest volumes of runoff, followed by the factor vegetation cover (maximum values at Level 4) (Table 5). Earlier studies showed that surface runoff depth is sensitive to the plot size and type of vegetation (Herweg and Ludi, 1999; Kort et al., 1998; Zuazo and Pleguezuelo, 2008). The optimum condition for maximum C and N losses were found to be $SiltOM_4$-VC_2-SS_4-RI_4-DLL_1 and $SiltOM_4$-VC_2-SS_4-RI_4-DLL_1 respectively (Table 5). The results indicate that rainfall intensity was the main factor that most influenced the sediment yield, runoff, C and N losses in the study area followed by vegetation cover and then slope steepness.

Table 4: The S/N ratio of each experiment resulting from a different combination of factors and levels.

Factors/ Plot	Combination of levels					Silt OM (%)	vegetation cover (%)	Slope steepness (%)	Rainfall intensity (mm min^{-1})	Depth to loamy layer (cm)	S/N			
	Silt OM	VC	SS	RI	DLL						Sediment yield	Runoff	C	N
1	1	1	1	1	1	>20	1-5	<1	<2.5	<40	36.08	16.53	1.65	-19.47
2	1	2	2	2	2	>20	0	1-3	2.7-3.3	40-55	41.98	19.05	10.35	-11.20
3	1	3	3	3	3	>20	10-15	3-5	3.4-4	55-70	45.47	24.62	13.96	-8.48
4	1	4	4	4	4	>20	>15	>5	>4	>70	46.70	27.42	17.71	-3.72
5	2	1	2	3	4	18-20	1-5	1-3	3.4-4	>70	46.31	17.70	11.96	-10.69
6	2	2	1	4	3	18-20	0	<1	>4	55-70	49.35	26.12	17.55	-4.56
7	2	3	4	1	2	18-20	10-15	>5	<2.5	40-55	43.60	19.87	9.65	-12.44
8	2	4	3	2	1	18-20	>15	3-5	2.7-3.3	<40	45.95	24.87	11.01	-10.35
9	3	1	3	4	2	16-18	1-5	3-5	>4	40-55	51.39	25.48	11.43	-10.58
10	3	2	4	3	1	16-18	0	>5	3.4-4	<40	53.97	26.21	21.59	-0.81
11	3	3	1	2	4	16-18	10-15	<1	2.7-3.3	>70	44.75	21.98	13.13	-9.09
12	3	4	2	1	3	16-18	>15	1-3	<2.5	55-70	35.63	18.42	6.02	-15.45
13	4	1	4	2	3	<16	1-5	>5	2.7-3.3	55-70	50.18	16.31	12.41	-8.20
14	4	2	3	1	4	<16	0	3-5	<2.5	>70	47.97	20.32	13.99	-8.54
15	4	3	2	4	1	<16	10-15	1-3	>4	<40	51.18	24.95	21.05	-0.46
16	4	4	1	3	2	<16	>15	<1	3.4-4	40-55	41.52	23.76	15.01	-7.19

Table 5: Mean S/N ratio response table for the investigated experimental factors

Output Parameter	Experimental factors	Mean S/N ratio				Delta	Rank
		Level 1	Level 2	Level 3	Level 4		
Sediment Yield	Silt+Organic material	42.56	46.30	46.44	**47.71**	5.15	4
	Vegetation Cover	45.99	**48.32**	46.25	42.45	5.87	2
	Slope Steepness	42.92	43.78	47.69	**48.61**	5.69	3
	Rainfall Intensity	40.82	45.71	46.82	**49.65**	8.83	1
	Depth to Loamy Layer	**46.79**	44.62	45.16	46.43	2.17	5
Runoff	Silt+ Organic material	21.91	22.14	**23.02**	21.34	1.69	5
	Vegetation Cover	19.01	22.93	22.86	**23.62**	4.61	2
	Slope Steepness	22.1	20.03	**23.82**	22.45	3.79	3
	Rainfall Intensity	18.79	20.56	23.07	**25.99**	7.21	1
	Depth to Loamy Layer	**23.14**	22.04	21.37	21.86	1.78	4
Carbon	Silt+ Organic material	10.92	12.54	12.91	**15.75**	4.83	3
	Vegetation Cover	9.36	**15.74**	14.58	12.44	6.37	2
	Slope Steepness	11.83	12.48	12.60	**15.21**	3.37	4
	Rainfall Intensity	7.83	11.73	15.50	**17.07**	9.24	1
	Depth to Loamy Layer	13.83	11.61	12.49	**14.20**	2.59	5
Nitrogen	Silt+ Organic material	-10.72	-9.51	-8.98	**-6.10**	4.61	3
	Vegetation Cover	-12.24	**-6.28**	-7.62	-9.18	5.95	2
	Slope Steepness	-10.08	-9.45	-9.49	**-6.29**	3.78	4
	Rainfall Intensity	-13.97	-9.71	-6.79	**-4.83**	9.14	1
	Depth to Loamy Layer	**-7.77**	-10.35	-9.17	-8.01	2.58	5

3.5. Percentage contribution of the experimental factors to sediment yield, runoff, C and N losses

ANOVA was used to estimate the contribution of the individual factors to sediment yield, runoff, C and N losses (Table 6). Rainfall intensity contributed most strongly to sediment yield (40.55 %) followed by slope steepness (23.76 %) and vegetation cover (17.73 %). (Peng and Wang, 2012) indicated that soil loss is positively related to rainfall events with high antecedent precipitations. The slope gradient can be more important than vegetation cover because of its relation with the

underlying geological formations resulting in varying soil characteristics. In consequence, slope gradients are related to soil moisture and hence the soil's susceptibility to soil detachment. Vegetation cover yields higher soil moisture at low to moderate slopes but it falls sharply at steeper slopes as soil permeability decreases that increases runoff till a threshold slope, moreover, the flow velocity becomes larger with increasing slope gradient due to increasing shear stress (Defersha and Melesse, 2012). The impact duration of runoff on steeper slopes becomes smaller and hence it weakens the protecting effect of surface seal, increasing the impact of rainfall splashing on the soil surface (Zhao et al., 2015). It produces more detachment of soil particles and transportation. However, the sum of silt content and organic material only contributes 14.77 % to sediment yield. (Ziadat and Taimeh, 2013a) showed a significant correlation between the ultimate infiltration rate and soil properties such as organic matter (R = 0.48) and silt content (R = 0.72). The low contribution of silt and organic matter to our results is most likely related to their comparatively low variation among measurement plots and due to the high content of organic matter that is varying from 2.3 to 2.4 % among the test plots. The high organic matter improves the aggregate stability, reduces the bulk density, and increases moisture retention and soil shear strength that helps in soil stability and resistance against erosion (Ekwue, 1990). Previous studies also concluded that aggregate stability is closely and negatively related to the soil detachment from field experiments under rainfall simulators on micro plots (Roth et al., 1987; Van Dijk et al., 1996). The factor of least importance in our study was the depth to the loamy layer (DLL) (3.17 %). This can be explained by the fact that the loamy layer with low permeability generally starts at relatively deep depths (lowest depth approximately 38 cm) and at many locations sand-filled pre-glacial ice cracks with higher permeability were observed in the loamy layer (Kühn, 2003). Therefore, differences in permeability and water storage capacity (risk of waterlogged soils) between experimental plots were probably relatively low. ANOVA results for the nitrogen (N) and carbon (C) content of sediment yield were similar (Table 6). As for sediment yield, rainfall intensity contributed most to the overall variation of C and N contents. The respective percentage contribution of rainfall intensity, vegetation cover, SiltOM content, slope and depth to loamy layer was 51.70%, 21.50 %, 12.55 %, 9.63 % and 4.62 % respectively for Nitrogen content and 52.31 %, 24.07 %, 12.39 %, 6.81 % and 4.41 % respectively for Carbon content. Runoff was mostly influenced by rainfall intensity (55.45 %) followed by vegetation cover, slope, depth to loamy layer, and SiltOM content. The respective contribution was 55.45 %, 24.71 %, 3.18 %, and 2.78 % (Table 6), agreeing with the findings of (Kirkby et al., 2004). The stronger impact of vegetation

cover compared with the slope can be explained by the stronger variability of vegetation cover at different soil management stages during the experimental period in the study area. In addition, at different slope levels varying soil compositions and moisture content affect the potential of surface runoff.

Table 6: Percentage contribution of each factor (ρF %) for the different output parameters as estimated by ANOVA

Output Parameters	ρ_F %				
	SiltOM	**Vegetation cover**	**Slope steepness**	**Rainfall intensity**	**Depth to Loamy Layer**
Sediment yield	14.77	17.74	23.77	**40.56**	3.17
Runoff	2.78	24.71	13.88	**55.45**	3.18
Nitrogen content	12.55	21.50	9.63	**51.70**	4.62
Carbon content	12.39	24.07	6.81	**52.31**	4.41

3.6.Linear regression models

Linear regression models are used to predict sediment yield, runoff, as well as C and N losses as a function of Silt + OM, vegetation cover, slope, rainfall intensity, and depth to the loamy layer. No transformation has been performed on the response variables. The estimated regression models are shown in the Eqns. (8-11).

Sediment yield = -7.2 + 40.9 SiltOM - 35.1 VC + 46.9 Slope + 58.6 RI - 18.4 DLL

(R^2 = 82.53) (8)

Runoff = 0.10 - 0.341 SiltOM + 1.807 VC + 0.933 Slope + 3.743 RI - 0.641 DLL

(R^2 = 79.66) (9)

C = -2.08 + 0.810 SiltOM + 0.371 VC + 0.446 Slope + 1.736 RI - 0.440 DLL

(R^2 = 60.97) (10)

N = -0.172 + 0.0629 SiltOM + 0.0299 VC + 0.0445 Slope + 0.1373 RI - 0.0381 DLL

(R^2 = 62.13) (11)

Where sediment yield, runoff depth, C and N are g m^{-2}, SiltOM and VC are %.

The capability of these empirical regression models was checked by using the coefficient of determination R^2. Regression models for sediment yield, runoff, carbon, and nitrogen yielded R^2 values of 82.53 %, 79.66 %, 60.97 %, and 62.13 % respectively. Residual plots (Fig. 7 A, B, C & D) indicate that residuals are independent and normally distributed. Sediment yield is positively related to SiltOM but runoff depth is negatively related. This indicates that a high amount of SiltOM would increase the erodibility of the soil but would reduce the runoff rate. This is also evident from Fig. 5A and B. The sediment yield is more sensitive to SiltOM compared to runoff. Coefficients of SiltOM for C and N losses show a positive relationship. C was more responsive to SiltOM as compared to N. It is suggested to have further research to find a threshold point for SiltOM in the soil to achieve the lowest sediment yield and runoff. Fig. 8 represents the scatter plot of predicted vs observed values with high R^2. The shaded band is a pointwise 95 % confidence interval on the fitted values. These results confirm the ability of the Taguchi method for the prediction of soil erosion in response to different combinations of factors/levels. The regression equation for sediment yield was further applied to predict sediment yields across the entire field for identifying areas within the field that have a higher susceptibility to soil erosion (Fig. 9).

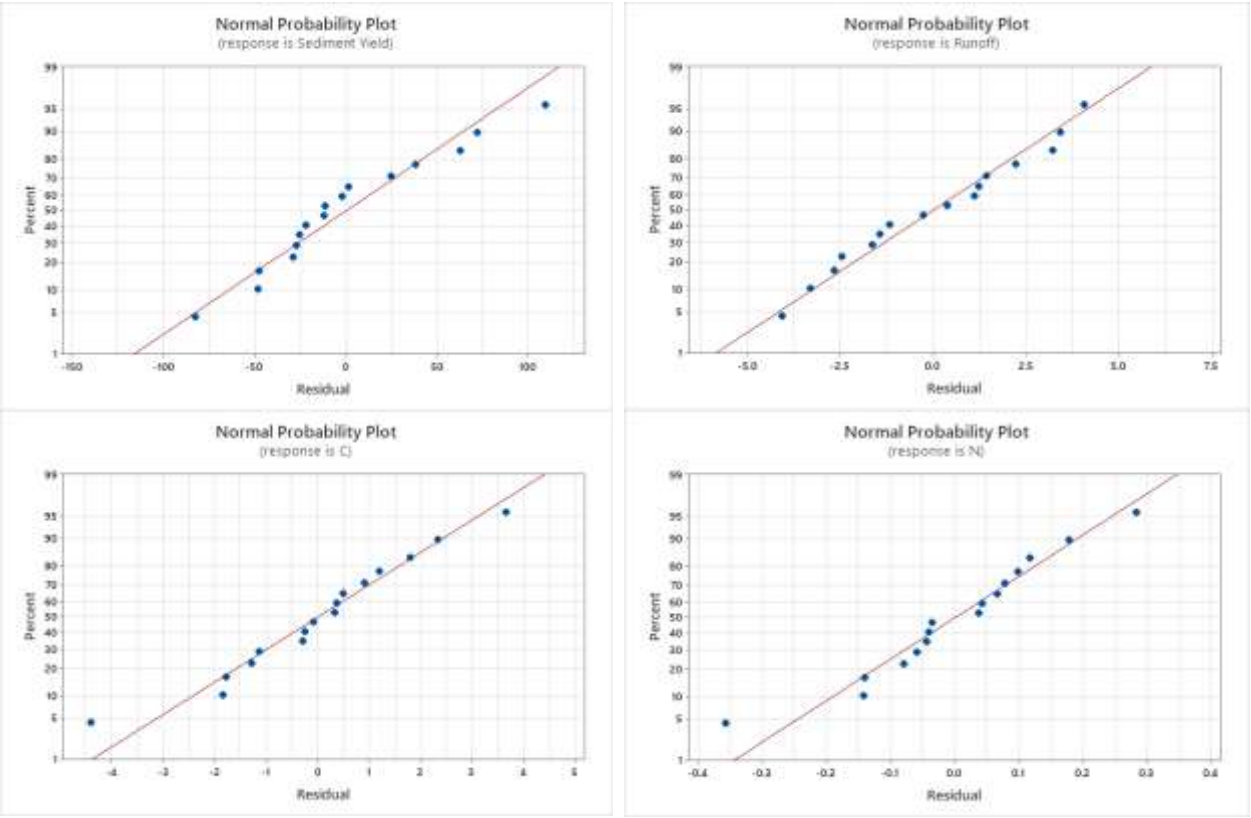


Fig. 7: Distribution of residuals of the regression models for sediment yield, runoff, carbon, and nitrogen

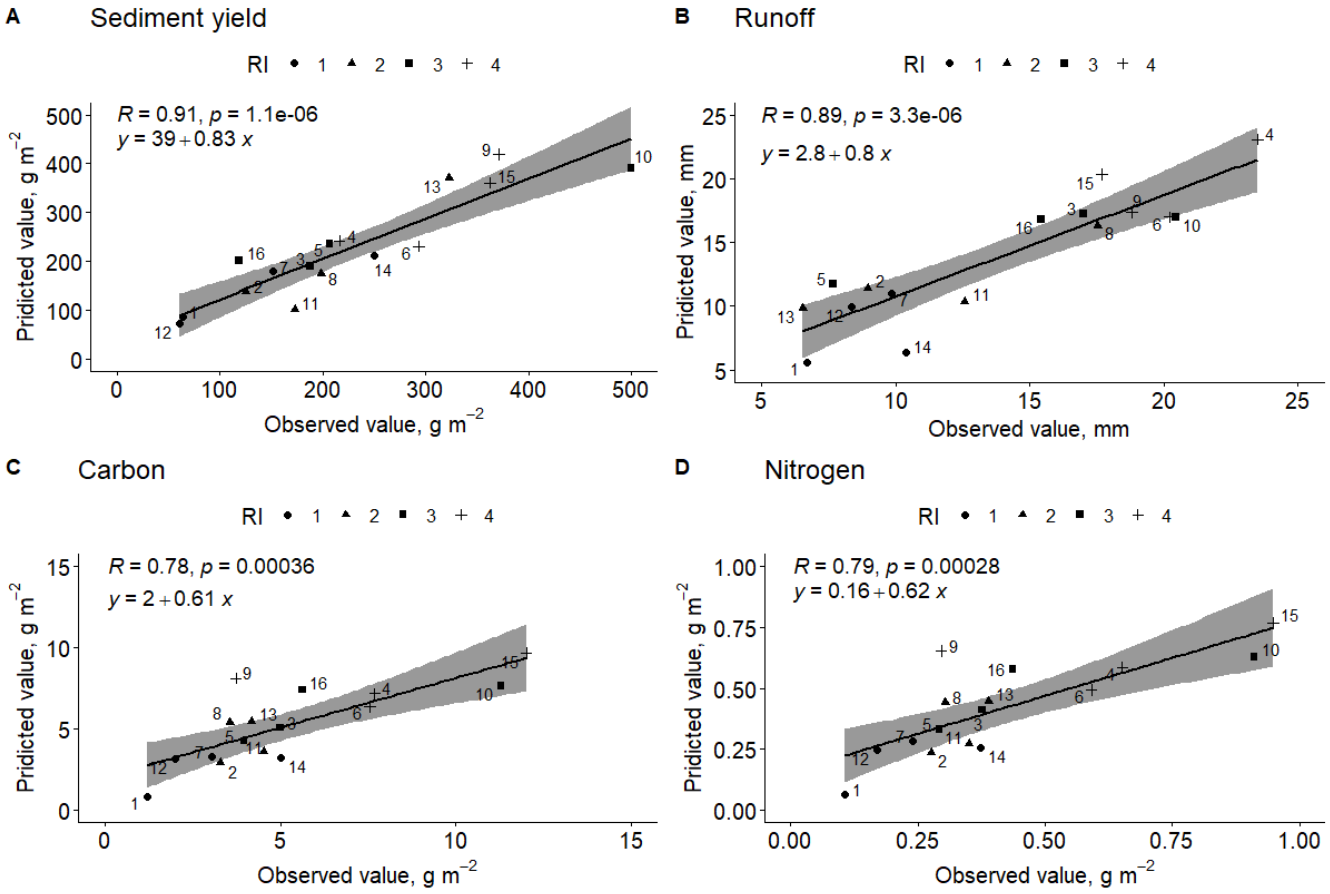
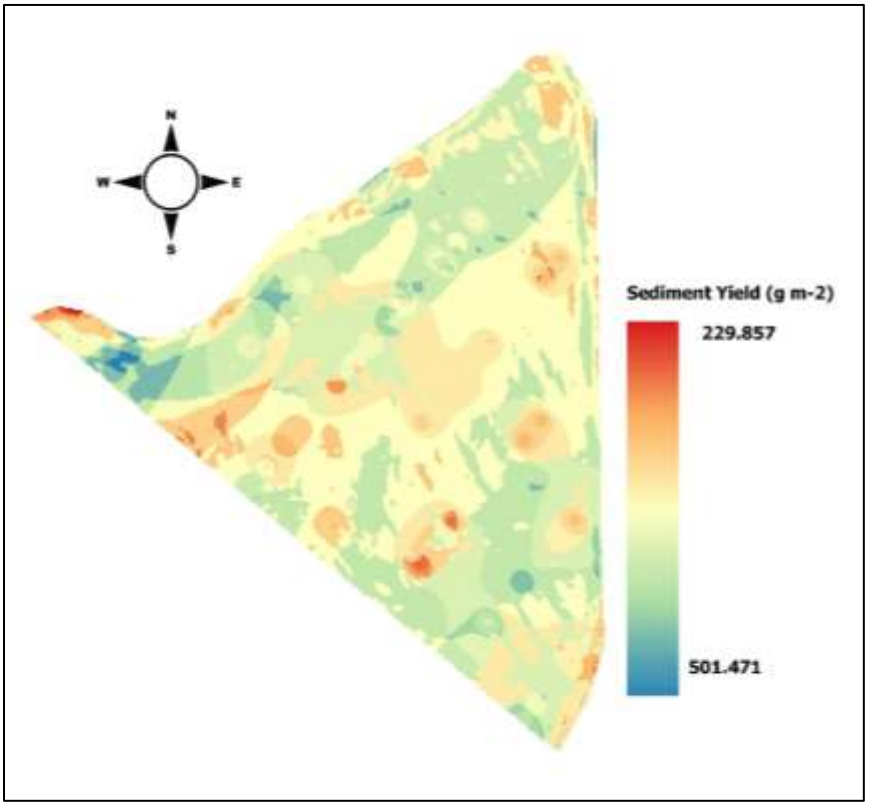


Fig. 8: Predicted versus observed sediment yield, runoff depth, carbon, and nitrogen losses



719

720

721 **Fig. 9: Identification of potential soil erosion risk areas**

722 **4. Conclusion**

723 Different scenarios were tested with 16 effective simulated rainfall events under different rainfall
724 intensities, vegetation cover, heterogeneous in-field slope, and soil conditions. The results
725 indicated that runoff, soil, and CN losses increase with increasing rainfall intensity. it was observed
726 that sediment yield, overland flow, CN content were greatly affected by rainfall intensity having a
727 contribution of 40.56 %, 55.45 %, 51.70 %, and 52.31 % respectively among the other factors.
728 However, the least contributing factor was depth to loamy layer for all output variables except for
729 surface runoff. The results show that the worst conditions among 16 plots were at $SiltOM_3$-VC_2-
730 SS_4-RI_3-DLL_1 for sediment yield. However, predicted experimental factors for the highest
731 sediment yield were found with the factor combination $SiltOM_4$-VC_2-SS_4-RI_4-DLL_1 and the lowest
732 sediment yield was observed with the factor combination $SiltOM_1$-VC_4-SS_1-RI_1-DLL_2. The
733 threshold rainfall intensity for soil erosion was 2.5 mm min^{-1}. VC and DLL are inversely correlated
734 with sediment yield, while SiltOM, slope, and rainfall intensity are directly correlated.

735 The surface runoff was negatively related to SiltOM and DLL, but the vegetative cover, slope, and
736 rainfall intensity positively affect the runoff. Regarding, C and N, except the DLL, other factors
737 show a positive correlation. Based on the experimental results, statistical regression models were
738 developed, which were applied for identifying the erosion risk areas at the field scale. The applied
739 workflow allowed for efficiently predicting soil erosion and identifying areas susceptible to soil
740 loss at a high spatial resolution. The study approved the capabilities of Taguchi's fractional

factorial design to efficiently analyze the response of soil erosion to dominant driving factors and detect and quantify in-field heterogeneity of erosion risk areas. The statistical models generated in this study can be used by environmental agencies and farmers for spatially explicit application of erosion control measures within fields with high spatial heterogeneity. Further, it is suggested that combining GIS with such numerical models can give great benefits for water quality control and soil management on larger scales with intensive spatial heterogeneous field conditions.

CRediT authorship contribution statement

Conceptualization, A.R., T.G., M.H.R., and H.A.; methodology, A.R., M.H.R., T.G., and H.A.; resource and data curation, A.R., T.G., and H.A., writing-original draft preparation, A.R.; writing-review and editing, T.G., M.H.R., H.A., and A.R.; visualization, M.H.R., H.A., and T.G.; supervision, T.G.; project administration, T.G.; funding acquisition, T.G., H.A.; All authors have read and agreed to the published version of the manuscript.

Funding

This research was funded by the German Federal Ministry of Education and Research (BMBF) through the Digital Agriculture Knowledge and Information System (DAKIS) Project, grant number 031B0729E, and by the Deutsche Forschungsgemeinschaft (DFG, German Research Foundation) under Germany's Excellence Strategy-EXC 2070-390732324 (PhenoRob). The APC was funded by the Crop Science Group, University of Bonn, Germany.

Declaration of competing interest

The authors declare that they have no known competing financial interests or personal relationships that could have appeared to influence the work reported in this paper.

References

Aga, A.O., Melesse, A.M., Chane, B., 2020. An alternative empirical model to estimate watershed sediment yield based on hydrology and geomorphology of the basin in data-scarce rift VALLEY lake regions, Ethiopia. Geosci. 10. https://doi.org/10.3390/geosciences10010031

Albaladejo Montoro, J., Stocking, M., 1989. Comparative evaluation of two models in predicting storm soil loss from erosion plots in semi-arid Spain. Catena 16, 227–236. https://doi.org/10.1016/0341-8162(89)90010-6

Anh, P.T.Q., Gomi, T., MacDonald, L.H., Mizugaki, S., Van Khoa, P., Furuichi, T., 2014. Linkages among land use, macronutrient levels, and soil erosion in northern Vietnam: A plot-scale study. Geoderma 232–234, 352–362. https://doi.org/10.1016/j.geoderma.2014.05.011

Awadhwal, N.K., Thierstein, G.E., 1985. Soil crust and its impact on crop establishment: A review. Soil Tillage Res. 5, 289–302. https://doi.org/10.1016/0167-1987(85)90021-2

Barthès, B., Roose, E., 2002. Aggregate stability as an indicator of soil susceptibility to runoff and erosion; validation at several levels. Catena 47, 133–149. https://doi.org/10.1016/S0341-8162(01)00180-1

779 Baruah, S., Ramalingam, K., Kannan, B., Kaliaperumal, R., 2019. Soil erodibility estimation and
780 its correlation with soil properties in Coimbatore district Soil erodibility estimation and its
781 correlation with soil properties in Coimbatore district. Int. J. Chem. Stud. 7, 3327–3332.

782 Benjeddou, O., Soussi, C., Jedidi, M., Benali, M., 2017. Experimental and theoretical study of the
783 effect of the particle size of limestone fillers on the rheology of self-compacting concrete. J.
784 Build. Eng. 10, 32–41. https://doi.org/10.1016/J.JOBE.2017.02.003

785 Brakensiek, D.L., Rawls, W.J., 1994. Soil containing rock fragments: effects on infiltration.
786 CATENA 23, 99–110. https://doi.org/10.1016/0341-8162(94)90056-6

787 Burch, G.J., Moore, I.D., Burns, J., 1989. Soil hydrophobic effects on infiltration and catchment
788 runoff. Hydrol. Process. 3, 211–222. https://doi.org/10.1002/HYP.3360030302

789 Buttle, J.M., Turcotte, D.S., 1999. Runoff processes on a forested slope on the Canadian shield.
790 Nord. Hydrol. 30, 1–20. https://doi.org/10.2166/nh.1999.0001

791 Cerdà, A., Lucas-Borja, M.E., Franch-Pardo, I., Úbeda, X., Novara, A., López-Vicente, M.,
792 Popović, Z., Pulido, M., 2021. The role of plant species on runoff and soil erosion in a
793 Mediterranean shrubland. Sci. Total Environ. 799, 149218.
794 https://doi.org/10.1016/j.scitotenv.2021.149218

795 Cerdan, O., Govers, G., Le Bissonnais, Y., Van Oost, K., Poesen, J., Saby, N., Gobin, A., Vacca,
796 A., Quinton, J., Auerswald, K., Klik, A., Kwaad, F.J.P.M., Raclot, D., Ionita, I., Rejman, J.,
797 Rousseva, S., Muxart, T., Roxo, M.J., Dostal, T., 2010. Rates and spatial variations of soil
798 erosion in Europe: A study based on erosion plot data. Geomorphology 122, 167–177.
799 https://doi.org/10.1016/j.geomorph.2010.06.011

800 Chmelová, R., Šarapatka, B., 2002. Soil erosion by water: Contemporary research methods and
801 their use. Geographica 37, 23–30.

802 Chou, C.S., Yang, R.Y., Chen, J.H., Chou, S.W., 2010. The optimum conditions for preparing the
803 lead-free piezoelectric ceramic of Bi0.5Na0.5TiO3 using the Taguchi method. Powder
804 Technol. 199, 264–271. https://doi.org/10.1016/j.powtec.2010.01.015

805 Cox, N.J., Warburton, J., Armstrong, A., Holliday, V.J., 2008. Fitting concentration and load
806 rating curves with generalized linear models. Earth Surf. Process. Landforms 33, 25–39.
807 https://doi.org/10.1002/ESP.1523

808 De Jonge, L.W., Moldrup, P., Jacobsen, O.H., 2007. Soil-water content dependency of water
809 repellency in soils. Soil Sci. 172, 577–588. https://doi.org/10.1097/SS.0B013E318065C090

810 Defersha, M.B., Melesse, A.M., 2012. Effect of rainfall intensity, slope and antecedent moisture
811 content on sediment concentration and sediment enrichment ratio. Catena 90, 47–52.
812 https://doi.org/10.1016/j.catena.2011.11.002

813 Deng, L., Zhang, L., Fan, X., Sun, T., Fei, K., Ni, L., 2019. Effects of rainfall intensity and slope
814 gradient on runoff and sediment yield from hillslopes with weathered granite. Environ. Sci.
815 Pollut. Res. 26, 32559–32573. https://doi.org/10.1007/s11356-019-06486-z

816 Donjadee, S., Chinnarasri, C., 2012. Effects of rainfall intensity and slope gradient on the
817 application of vetiver grass mulch in soil and water conservation. Int. J. Sediment Res. 27,
818 168–177. https://doi.org/10.1016/S1001-6279(12)60025-0

819 Duiker, S.W., Flanagan, D.C., Lal, R., 2001. Erodibility and infiltration characteristics of five
820 major soils of southwest Spain. Catena 45, 103–121. https://doi.org/10.1016/S0341-
821 8162(01)00145-X

822 Dunjó, G., Pardini, G., Gispert, M., 2004. The role of land use-land cover on runoff generation
823 and sediment yield at a microplot scale, in a small Mediterranean catchment. J. Arid
824 Environ. 57, 239–256. https://doi.org/10.1016/S0140-1963(03)00097-1

825 Ekwue, E.I., 1990. Organic-matter effects on soil strength properties. Soil Tillage Res. 16, 289–
826 297. https://doi.org/10.1016/0167-1987(90)90102-J

827 Eslamian, S., 2014. Handbook of engineering hydrology: Modeling, climate change, and
828 variability. Handb. Eng. Hydrol. Model. Clim. Chang. Var. 1–615.
829 https://doi.org/10.1201/b16683

830 Fernández-Gálvez, J., Barahona, E., Mingorance, M.D., 2008. Measurement of infiltration in
831 small field plots by a portable rainfall simulator: Application to trace-element mobility.
832 Water. Air. Soil Pollut. 191, 257–264. https://doi.org/10.1007/s11270-008-9622-2

833 Gomi, T., Sidle, R.C., Ueno, M., Miyata, S., Kosugi, K., 2008. Characteristics of overland flow
834 generation on steep forested hillslopes of central Japan. J. Hydrol. 361, 275–290.
835 https://doi.org/10.1016/J.JHYDROL.2008.07.045

836 Grismer, M.E., 2012. Modélisation de l'érosion pour la gestion des terres dans le bassin du lac
837 Tahoe, Etats-Unis: scalance depuis les parcelles jusqu'aux bassins versants forestiers.
838 Hydrol. Sci. J. 57, 878–900. https://doi.org/10.1080/02626667.2012.685170

839 Gross, C.M., Angle, J.S., Hill, R.L., Welterlen, M.S., 1991. Runoff and Sediment Losses from
840 Tall Fescue under Simulated Rainfall. J. Environ. Qual. 20, 604–607.
841 https://doi.org/10.2134/jeq1991.00472425002000030017x

842 Guidry, A.R., Schindler, F. V., German, D.R., Gelderman, R.H., Gerwing, J.R., 2006. Using
843 Simulated Rainfall to Evaluate Field and Indoor Surface Runoff Phosphorus Relationships.
844 J. Environ. Qual. 35, 2236–2243. https://doi.org/10.2134/jeq2006.0156

845 Guo, Z., Ma, M., Cai, C., Wu, Y., 2018. Combined effects of simulated rainfall and overland
846 flow on sediment and solute transport in hillslope erosion. J. Soils Sediments 18, 1120–
847 1132. https://doi.org/10.1007/s11368-017-1868-0

848 He, Z., Jia, G., Liu, Z., Zhang, Z., Yu, X., Xiao, P., 2020. Field studies on the influence of
849 rainfall intensity, vegetation cover and slope length on soil moisture infiltration on typical
850 watersheds of the Loess Plateau, China. Hydrol. Process. 34, 4904–4919.
851 https://doi.org/10.1002/hyp.13892

852 Heiskanen, J., 2008. Comparison of three methods for determining the particle density of soil
853 with liquid pycnometers. http://dx.doi.org/10.1080/00103629209368633 23, 841–846.
854 https://doi.org/10.1080/00103629209368633

855 Hermansen, C., Moldrup, P., Müller, K., Knadel, M., Jonge, L.W. de, 2019. The Relation
856 between Soil Water Repellency and Water Content Can Be Predicted by Vis-NIR
857 Spectroscopy. Soil Sci. Soc. Am. J. 83, 1616–1627.
858 https://doi.org/10.2136/SSSAJ2019.03.0092

Herweg, K., Ludi, E., 1999. The performance of selected soil and water conservation measures - Case studies from Ethiopia and Eritrea. Catena 36, 99–114. https://doi.org/10.1016/S0341-8162(99)00004-1

Holz, M., Augustin, J., 2021. Erosion effects on soil carbon and nitrogen dynamics on cultivated slopes: A meta-analysis. Geoderma 397, 115045. https://doi.org/10.1016/J.GEODERMA.2021.115045

Hrabovskỳ, A., Dlapa, P., Cerdà, A., Kollár, J., 2020. The impacts of vineyard afforestation on soil properties,water repellency and near-saturated infiltration in the little carpathians mountains. Water 12, 2550. https://doi.org/10.3390/w12092550

Huang, R., Huang, L., He, B., Zhou, L., Wang, F., 2012. Effects of slope forest and grass vegetation on reducing rainfall-runoff erosivity in Three Gorges Reservoir Region. Nongye Gongcheng Xuebao/Transactions Chinese Soc. Agric. Eng. 28, 70–76. https://doi.org/10.3969/j.issn.1002-6819.2012.09.012

Ihinegbu, C., Ogunwumi, T., 2021. Multi-criteria modelling of drought: a study of Brandenburg Federal State, Germany. Model. Earth Syst. Environ. 1, 3. https://doi.org/10.1007/s40808-021-01197-2

Issaka, S., Ashraf, M.A., 2017. Impact of soil erosion and degradation on water quality: a review. https://doi.org/10.1080/24749508.2017.1301053 1, 1–11. https://doi.org/10.1080/24749508.2017.1301053

J. R. Williams, C. A. Jones, P. T. Dyke, 1984. A Modeling Approach to Determining the Relationship Between Erosion and Soil Productivity. Trans. ASAE 27, 0129–0144. https://doi.org/10.13031/2013.32748

Jahun, B.G., Ibrahim, R., Dlamini, N.S., Musa, S.M., 2015. Review of Soil Erosion Assessment using RUSLE Model and GIS. J. Biol. Agric. Healthc. 5, 36–47.

Jebari, S., Berndtsson, R., Bahri, A., Boufaroua, M., 2008. Exceptional Rainfall Characteristics Related to Erosion Risk in Semiarid Tunisia. Open Hydrol. J. 2, 25–33. https://doi.org/10.2174/1874378100802010025

Jourgholami, M., Karami, S., Tavankar, F., Lo Monaco, A., Picchio, R., 2021. Effects of slope gradient on runoff and sediment yield on machine-induced compacted soil in temperate forests. Forests 12, 1–19. https://doi.org/10.3390/f12010049

Jourgholami, M., Labelle, E.R., 2020. Effects of plot length and soil texture on runoff and sediment yield occurring on machine-trafficked soils in a mixed deciduous forest. Ann. For. Sci. 77, 1–11. https://doi.org/10.1007/s13595-020-00938-0

Kamphorst, A., 1987. A small rainfall simulator for the determination of soil erodibility. Netherlands J. Agric. Sci. 35, 407–415. https://doi.org/10.18174/NJAS.V35I3.16735

Kandel, D.D., Western, A.W., Grayson, R.B., Turral, H.N., 2004. Process parameterization and temporal scaling in surface runoff and erosion modelling. Hydrol. Process. 18, 1423–1446. https://doi.org/10.1002/hyp.1421

Keating, B.A., Carberry, P.S., Hammer, G.L., Probert, M.E., Robertson, M.J., Holzworth, D., Huth, N.I., Hargreaves, J.N.G., Meinke, H., Hochman, Z., McLean, G., Verburg, K., Snow,

V., Dimes, J.P., Silburn, M., Wang, E., Brown, S., Bristow, K.L., Asseng, S., Chapman, S., McCown, R.L., Freebairn, D.M., Smith, C.J., 2003. An overview of APSIM, a model designed for farming systems simulation. Eur. J. Agron. 18, 267–288. https://doi.org/10.1016/S1161-0301(02)00108-9

Kirkby, M.J., Jones, R., Irvine, B., Gobin, A., Govers, G., Cerdan, O., Rompaey, A.J.J. Van, Le Bissonnais, Y., Daroussin, J., King, D., Montanarella, L., Grimm, M., Vieillefont, V., Puigdefabregas, J., Boer, M., Kosmas, C., Yassoglou, N., Tsara, M., Mantel, S., Lynden, G.J. Van, Huting, J., 2004. Pan-European Soil Erosion Risk Assessment: The PESERA Map, Version 1 October 2003. Explanation of Special Publication Ispra 2004 No.73 (S.P.I.04.73), European Soil Bureau Research Report. Luxembourg.

Knadel, M., Masís-Meléndez, F., De Jonge, L.W., Moldrup, P., Arthur, E., Greve, M.H., 2016. Assessing Soil Water Repellency of a Sandy Field with Visible near Infrared Spectroscopy: http://dx.doi.org/10.1255/jnirs.1188 24, 215–224. https://doi.org/10.1255/JNIRS.1188

Knisel, W.G., Nicks, A.D., 1981. CREAMS: A Field Scale Model for Chemicals, Runoff, and Erosion from Agriculture Management System, 26th ed, United States. Science and Education Administration. Dept. of Agriculture, Science and Education Administration.

Kort, J., Collins, M., Ditsch, D., 1998. A review of soil erosion potential associated with biomass crops. Biomass and Bioenergy 14, 351–359. https://doi.org/10.1016/S0961-9534(97)10071-X

Krisnayanti, D.S., Bunganaen, W., Frans, J.H., Seran, Y.A., Legono, D., 2021. Curve number estimation for ungauged watershed in semiarid region. Civ. Eng. J. 7, 1070–1083. https://doi.org/10.28991/CEJ-2021-03091711

Krysanova, V., Hattermann, F., Wechsung, F., 2007. Implications of complexity and uncertainty for integrated modelling and impact assessment in river basins. Environ. Model. Softw. 22, 701–709. https://doi.org/10.1016/j.envsoft.2005.12.029

Kühn, P., 2003. Micromorphology and Late Glacial/Holocene genesis of Luvisols in Mecklenburg–Vorpommern (NE-Germany). CATENA 54, 537–555. https://doi.org/10.1016/S0341-8162(03)00129-2

Kusumandari, A., Satriagasa, M.C., Hadi Purwanto, R., Widayanti, W.T., 2021. Erosion Measurement by Using Rainfall Simulator at Grass Soil and after Harvested Soil in Wanagama, in: IOP Conference Series: Earth and Environmental Science. IOP Publishing. https://doi.org/10.1088/1755-1315/810/1/012053

L. D. Meyer, 1981. How Rain Intensity Affects Interrill Erosion. Trans. ASAE 24, 1472–1475. https://doi.org/10.13031/2013.34475

Lasanta, T., García-Ruiz, J.M., Pérez-Rontomé, C., Sancho-Marcén, C., 2000. Runoff and sediment yield in a semi-arid environment: The effect of land management after farmland abandonment. Catena 38, 265–278. https://doi.org/10.1016/S0341-8162(99)00079-X

Li, T., Zhao, L., Duan, H., Yang, Y., Wang, Y., Wu, F., 2020. Exploring the interaction of surface roughness and slope gradient in controlling rates of soil loss from sloping farmland on the Loess Plateau of China. Hydrol. Process. 34, 339–354. https://doi.org/10.1002/HYP.13588

Li, Y., Zhang, F., Yang, M., Zhang, J., Xie, Y., 2019. Impacts of biochar application rates and particle sizes on runoff and soil loss in small cultivated loess plots under simulated rainfall. Sci. Total Environ. 649, 1403–1413. https://doi.org/10.1016/j.scitotenv.2018.08.415

Li, Z., Liu, C., Dong, Y., Chang, X., Nie, X., Liu, L., Xiao, H., Lu, Y., Zeng, G., 2017. Response of soil organic carbon and nitrogen stocks to soil erosion and land use types in the Loess hilly–gully region of China. Soil Tillage Res. 166, 1–9. https://doi.org/10.1016/j.still.2016.10.004

Li, Z., Yu, X., 2012. Characteristics of surface runoff and its influencing factors on slope scale in rocky mountain area of northern Hebei province. Nongye Gongcheng Xuebao/Transactions Chinese Soc. Agric. Eng. 28, 109–116. https://doi.org/10.3969/J.ISSN.1002-6819.2012.17.016

Lin, J., Zhu, G., Wei, J., Jiang, F., Wang, M. kuang, Huang, Y., 2018. Mulching effects on erosion from steep slopes and sediment particle size distributions of gully colluvial deposits. CATENA 160, 57–67. https://doi.org/10.1016/J.CATENA.2017.09.003

Liu, D., She, D., Yu, S., Shao, G., Chen, D., 2015. Rainfall intensity and slope gradient effects on sediment losses and splash from a saline-sodic soil under coastal reclamation. Catena 128, 54–62. https://doi.org/10.1016/j.catena.2015.01.022

Liu, Singh, 2004. Effect of Microtopography, Slope Length and Gradient, and Vegetative Cover on Overland Flow through Simulation. J. Hydrol. Eng. 9, 375–382. https://doi.org/10.1061/(ASCE)1084-0699(2004)9:5(375)

Liu, Y., Xin, Y., Xie, Y., Wang, W., 2019. Effects of slope and rainfall intensity on runoff and soil erosion from furrow diking under simulated rainfall. Catena 177, 92–100. https://doi.org/10.1016/j.catena.2019.02.004

Loch, R.J., 2000. Effects of vegetation cover on runoff and erosion under simulated rain and overland flow on a rehabilitated site on the Meandu Mine, Tarong, Queensland. Soil Res. 38, 299–312. https://doi.org/10.1071/SR99030

Lu, J., Zheng, F., Li, G., Bian, F., An, J., 2016. The effects of raindrop impact and runoff detachment on hillslope soil erosion and soil aggregate loss in the Mollisol region of Northeast China. Soil Tillage Res. 161, 79–85. https://doi.org/10.1016/J.STILL.2016.04.002

M. Sheklabadi, H. Khademi, A. H. Charkhabi, 2012. Runoff and Sediment Yield in Soils Developed on Different Parent Materials in the Golabad Watershed, Ardestan. J. Sci. Technol. Agric. Nat. Resour. 7, 101–245.

Meena, R.S., Lal, R., Yadav, G.S., 2020. Long-term impacts of topsoil depth and amendments on soil physical and hydrological properties of an Alfisol in central Ohio, USA. Geoderma 363, 114164. https://doi.org/10.1016/J.GEODERMA.2019.114164

Meng, Q., Fu, B., Tang, X., Ren, H., 2007. Effects of land use on phosphorus loss in the hilly area of the Loess Plateau, China. Environ. Monit. Assess. 2007 1391 139, 195–204. https://doi.org/10.1007/S10661-007-9826-8

Meyer, L.D., Harmon, W.C., 1989. How row-sideslope length and steepness affect sideslope erosion. Trans. Am. Soc. Agric. Eng. 32, 639–644. https://doi.org/10.13031/2013.31050

Michel, E., Majdalani, S., Di-Pietro, L., 2014. A novel conceptual framework for long-term leaching of autochthonous soil particles during transient flow. Eur. J. Soil Sci. 65, 336–347. https://doi.org/10.1111/ejss.12135

Mohamadi, M.A., Kavian, A., 2015. Effects of rainfall patterns on runoff and soil erosion in field plots. Int. Soil Water Conserv. Res. 3, 273–281. https://doi.org/10.1016/j.iswcr.2015.10.001

Nassif, S.H., Wilson, E.M., 1975. The influence of slope and rain intensity on runoff and infiltration. Hydrol. Sci. Bull. 20, 539–553. https://doi.org/10.1080/02626667509491586

Nearing, M.A., Simanton, J.R., Norton, L.D., Bulygin, S.J., Stone, J., 1999. Soil erosion by surface water flow on a stony, semiarid hillslope. Earth Surf. Process. Landforms 24, 677–686. https://doi.org/10.1002/(SICI)1096-9837(199908)24:8<677::AID-ESP981>3.0.CO;2-1

Nunes, A.N., de Almeida, A.C., Coelho, C.O.A., 2011. Impacts of land use and cover type on runoff and soil erosion in a marginal area of Portugal. Appl. Geogr. 31, 687–699. https://doi.org/10.1016/J.APGEOG.2010.12.006

Ouyang, W., Wu, Y., Hao, Z., Zhang, Q., Bu, Q., Gao, X., 2018. Combined impacts of land use and soil property changes on soil erosion in a mollisol area under long-term agricultural development. Sci. Total Environ. 613–614, 798–809. https://doi.org/10.1016/J.SCITOTENV.2017.09.173

P.U., I., A.A., O., O.C., C., I.I., E., M.M., M., 2017. Soil Erosion: A Review of Models and Applications. Int. J. Adv. Eng. Res. Sci. 4, 138–150. https://doi.org/10.22161/ijaers.4.12.22

Panagos, P., Katsoyiannis, A., 2019. Soil erosion modelling: The new challenges as the result of policy developments in Europe. Environ. Res. 172, 470–474. https://doi.org/10.1016/j.envres.2019.02.043

Pandey, A., Chowdary, V.M., Mal, B.C., 2007. Identification of critical erosion prone areas in the small agricultural watershed using USLE, GIS and remote sensing. Water Resour. Manag. 21, 729–746. https://doi.org/10.1007/s11269-006-9061-z

Parr, W.C., Taguchi, G., 1989. Introduction to Quality Engineering: Designing Quality into Products and Processes. Technometrics 31, 255. https://doi.org/10.2307/1268824

Peng, T., Wang, S. jie, 2012. Effects of land use, land cover and rainfall regimes on the surface runoff and soil loss on karst slopes in southwest China. CATENA 90, 53–62. https://doi.org/10.1016/J.CATENA.2011.11.001

Poulenard, J., Podwojewski, P., Janeau, J.L., Collinet, J., 2001. Runoff and soil erosion under rainfall simulation of Andisols from the Ecuadorian Páramo: Effect of tillage and burning. Catena 45, 185–207. https://doi.org/10.1016/S0341-8162(01)00148-5

Rainfall simulator - Field measurement equipment | Eijkelkamp [WWW Document], 2018. URL https://en.eijkelkamp.com/products/field-measurement-equipment/rainfall-simulator.html (accessed 10.20.21).

Ramezanpour, H., Esmaeilnejad, L., Akbarzadeh, A., 2010. Influence of soil physical and mineralogical properties on erosion variations in Marlylands of Southern Guilan Province, Iran. Int. J. Phys. Sci. 5, 365–378. https://doi.org/10.5897/IJPS.9000311

Ramos, M.C., Lizaga, I., Gaspar, L., Quijano, L., Navas, A., 2019. Effects of rainfall intensity and slope on sediment, nitrogen and phosphorous losses in soils with different use and soil hydrological properties. Agric. Water Manag. 226, 105789. https://doi.org/10.1016/j.agwat.2019.105789

Raza, A., Ahrends, H., Habib-Ur-Rahman, M., Gaiser, T., 2021. Modeling Approaches to Assess Soil Erosion by Water at the Field Scale with Special Emphasis on Heterogeneity of Soils and Crops. L. 2021, Vol. 10, Page 422 10, 422. https://doi.org/10.3390/LAND10040422

Renard, K.G., Foster, G.R., Weesies, G.A., Porter, J.P., 1991. RUSLE: revised universal soil loss equation. J. Soil Water Conserv. 46, 30–33.

Rieke-Zapp, D.H., Nearing, M.A., 2005. Slope Shape Effects on Erosion: A Laboratory Study. Soil Sci. Soc. Am. J. 69, 1463–1471. https://doi.org/10.2136/sssaj2005.0015

Roth, C.H., Vieira, M.J., Derpsch, R., Meyer, B., Frede, H. -G, 1987. Infiltrability of an Oxisol in Paraná, Brazil as Influenced by Different Crop Rotations. J. Agron. Crop Sci. 159, 186–191. https://doi.org/10.1111/j.1439-037X.1987.tb00084.x

Sadeghi, S.H., Kiani Harchegani, M., Asadi, H., 2017. Variability of particle size distributions of upward/downward splashed materials in different rainfall intensities and slopes. Geoderma 290, 100–106. https://doi.org/10.1016/j.geoderma.2016.12.007

Sepaskhah, A.R., Bazrafshan-Jahromi, A.R., 2006. Controlling Runoff and Erosion in Sloping Land with Polyacrylamide under a Rainfall Simulator. Biosyst. Eng. 93, 469–474. https://doi.org/10.1016/j.biosystemseng.2006.01.003

Sharpley, A., Kleinman, P., 2003. Effect of Rainfall Simulator and Plot Scale on Overland Flow and Phosphorus Transport. J. Environ. Qual. 32, 2172–2179. https://doi.org/10.2134/jeq2003.2172

Sivaiah, P., Chakradhar, D., 2019. Modeling and optimization of sustainable manufacturing process in machining of 17-4 PH stainless steel. Meas. J. Int. Meas. Confed. 134, 142–152. https://doi.org/10.1016/j.measurement.2018.10.067

Sosa-Pérez, G., MacDonald, L.H., 2017. Effects of closed roads, traffic, and road decommissioning on infiltration and sediment production: A comparative study using rainfall simulations. CATENA 159, 93–105. https://doi.org/10.1016/J.CATENA.2017.08.004

Srinivasan, M.S., Kleinman, P.J.A., Sharpley, A.N., Buob, T., Gburek, W.J., 2007. Hydrology of Small Field Plots Used to Study Phosphorus Runoff under Simulated Rainfall. J. Environ. Qual. 36, 1833–1842. https://doi.org/10.2134/jeq2007.0017

Sukartaatmadja, S., Sato, Y., Yamaji, E., Ishikawa, M., 2003. The Effect of Rainfall Intensity on Soil Erosion and Runoff for Latosol Soil in Indonesia. Indones. J. Agron. 31. https://doi.org/10.24831/jai.v31i2.1469

Sun, L., Zhou, J.L., Cai, Q., Liu, S., Xiao, J., 2021. Comparing surface erosion processes in four soils from the Loess Plateau under extreme rainfall events. Int. Soil Water Conserv. Res. 9, 520–531. https://doi.org/10.1016/J.ISWCR.2021.06.008

Syvitski, J.P.M., Kettner, A.J., 2008. Scaling sediment flux across landscapes. IAHS-AISH Publ.

149–156.

Taguchi, G., 1987. The System of Experimental Design: Engineering Methods to Optimize Quality and Minimize Costs , 1st ed, Response. Quality Resources.

Taguchi, G., 1986. Introduction to quality engineering : designing quality into products and processes. Quality Resources.

Tong Li, Dong, J., Yuan, W., 2020. Effects of Precipitation and Vegetation Cover on Annual Runoff and Sediment Yield in Northeast China: A Preliminary Analysis. Water Resour. 47, 491–505. https://doi.org/10.1134/S0097807820030173/FIGURES/10

Václavík, T., Lautenbach, S., Kuemmerle, T., Seppelt, R., 2013. Mapping global land system archetypes. Glob. Environ. Chang. 23, 1637–1647. https://doi.org/10.1016/j.gloenvcha.2013.09.004

Van Dijk, P.M., Van Der Zijp, M., Kwaad, F.J.P.M., 1996. Soil erodibility parameters under various cropping systems of maize. Hydrol. Process. 10, 1061–1067. https://doi.org/10.1002/(SICI)1099-1085(199608)10:8<1061::AID-HYP411>3.0.CO;2-V

Viney, N.R., Sivapalan, M., 1999. A conceptual model of sediment transport: Application to the Avon River Basin in Western Australia. Hydrol. Process. 13, 727–743. https://doi.org/10.1002/(SICI)1099-1085(19990415)13:5<727::AID-HYP776>3.0.CO;2-D

Wang, Y., Fan, J., Cao, L., Liang, Y., 2016. Infiltration and Runoff Generation Under Various Cropping Patterns in the Red Soil Region of China. L. Degrad. Dev. 27, 83–91. https://doi.org/10.1002/ldr.2460

Warrington, D., Shainberg, I., Agassi, M., Morin, J., 1989. Slope and Phosphogypsum's Effects on Runoff and Erosion. Soil Sci. Soc. Am. J. 53, 1201–1205. https://doi.org/10.2136/sssaj1989.03615995005300040035x

Wu, L., Peng, M., Qiao, S., Ma, X. yi, 2018a. Effects of rainfall intensity and slope gradient on runoff and sediment yield characteristics of bare loess soil. Environ. Sci. Pollut. Res. https://doi.org/10.1007/s11356-017-0713-8

Wu, L., Qiao, S., Peng, M., Ma, X., 2018b. Coupling loss characteristics of runoff-sediment-adsorbed and dissolved nitrogen and phosphorus on bare loess slope. Environ. Sci. Pollut. Res. 25, 14018–14031. https://doi.org/10.1007/s11356-018-1619-9

Yan, Y., Dai, Q., Yuan, Y., Peng, X., Zhao, L., Yang, J., 2018. Effects of rainfall intensity on runoff and sediment yields on bare slopes in a karst area, SW China. Geoderma 330, 30–40. https://doi.org/10.1016/j.geoderma.2018.05.026

Yost, J.L., Hartemink, A.E., 2019. Soil organic carbon in sandy soils: A review. Adv. Agron. 158, 217–310. https://doi.org/10.1016/BS.AGRON.2019.07.004

Yusuf, K., Omokore, S., Oyebode, O., Adebayo, K., 2016. Effect of vegetative cover and slope on soil loss by erosion using rainfall simulator. J. Res. For. Wildl. Environ. 8, 45–52.

Zambon, N., Johannsen, L.L., Strauss, P., Dostal, T., Zumr, D., Cochrane, T.A., Klik, A., 2021. Splash erosion affected by initial soil moisture and surface conditions under simulated rainfall. Catena 196, 104827. https://doi.org/10.1016/j.catena.2020.104827

Zapata, N., Salvador, R., Latorre, B., Paniagua, P., Medina, E.T., Playán, E., 2021. Effect of a growing maize canopy on solid-set sprinkler irrigation: kinetic energy dissipation and water partitioning. Irrig. Sci. 39, 329–346. https://doi.org/10.1007/S00271-020-00713-Z/FIGURES/10

Zhang, F., Yang, M., Li, Z., 2015. Feasibility analysis of replacing full factorial design with Taguchi method in mini-plot soil erosion experiments. Nongye Gongcheng Xuebao/Transactions Chinese Soc. Agric. Eng. 31, 1–9. https://doi.org/10.11975/J.ISSN.1002-6819.2015.13.001

Zhang, J.H., Wang, Y., Li, F.C., 2015. Soil organic carbon and nitrogen losses due to soil erosion and cropping in a sloping terrace landscape. Soil Res. 53, 87–96. https://doi.org/10.1071/SR14151

Zhao, Q., Li, D., Zhuo, M., Guo, T., Liao, Y., Xie, Z., 2015. Effects of rainfall intensity and slope gradient on erosion characteristics of the red soil slope. Stoch. Environ. Res. Risk Assess. 29, 609–621. https://doi.org/10.1007/S00477-014-0896-1/FIGURES/6

Zhong, R.-L., Zhang, P.-C., 2011. Experimental Study on Characteristics of Runoff and Erosional Sediment Yield on Purple Soil Slope. J. yangtze river Sci. Res. Inst. 28, 22–27.

Ziadat, F.M., Taimeh, A.Y., 2013a. Effect of rainfall intensity, slope, land use and antecedent soil moisture on soil erosion in an arid environment. L. Degrad. Dev. 24, 582–590. https://doi.org/10.1002/ldr.2239

Ziadat, F.M., Taimeh, A.Y., 2013b. Effect of rainfall intensity, slope, land use and antecedent soil moisture on soil erosion in an arid environment. L. Degrad. Dev. 24, 582–590. https://doi.org/10.1002/ldr.2239

Zuazo, V.H.D., Pleguezuelo, C.R.R., 2008. Soil-erosion and runoff prevention by plant covers. A review. Agron. Sustain. Dev. https://doi.org/10.1051/agro:2007062